HHS Public Access

Author manuscript

Nat Immunol. Author manuscript; available in PMC 2019 November 20.

Published in final edited form as:

Nat Immunol. 2019 June ; 20(6): 677–686. doi:10.1038/s41590-019-0396-z.

Toll-like receptors TLR2 and TLR4 block the replication of pancreatic β cells in diet-induced obesity

Yewei Ji[1,2,13], **Shengyi Sun**[2,10,13], **Neha Shrestha**[1], **Laurel B. Darragh**[2,11], **Jun Shirakawa**[3], **Yuan Xing**[4], **Yi He**[4], **Bethany A. Carboneau**[5], **Hana Kim**[2,12], **Duo An**[6], **Minglin Ma**[6], **Jose Oberhozler**[4], **Scott A. Soleimanpour**[7], **Maureen Gannon**[5], **Chengyang Liu**[8], **Ali Naji**[8], **Rohit N. Kulkarni**[3], **Yong Wang**[4], **Sander Kersten**[2,9], and **Ling Qi**[1,2,7,*]

[1]Department of Molecular and Integrative Physiology, University of Michigan Medical School, Ann Arbor, Michigan 48109, USA; [2]Division of Nutritional Sciences, Cornell University, Ithaca, New York 14853, USA; [3]Section of Islet Cell and Regenerative Biology, Joslin Diabetes Center, Department of Medicine, Brigham and Women's Hospital, Harvard Stem Cell Institute, Harvard Medical School, Boston, Massachusetts, USA; [4]Department of Surgery, University of Virginia, Charlottesville, Virginia 22908, USA; [5]Division of Diabetes, Endocrinology and Metabolism, Vanderbilt University Medical Center, Nashville, Tennessee 37232, USA; [6]Department of Biological and Environmental Engineering, Cornell University, Ithaca, New York 14853, USA; [7]Department of Internal Medicine, University of Michigan Medical School, Ann Arbor, Michigan 48105, USA; [8]Department of Surgery, Perelman School of Medicine at the University of Pennsylvania, Philadelphia, Pennsylvania 19104, USA; [9]Nutrition Metabolism and Genomics group, Wageningen University, Wageningen, The Netherlands; [10]Present address: Center for Molecular Medicine and Genetics, Department of Microbiology, Immunology, and Biochemistry, Wayne State University School of Medicine, Detroit, Michigan, USA; [11]Present address: Department of Radiation Oncology, School of Medicine, University of Colorado, Aurora, Colorado 80045, USA; [12]Present address: XBiotech USA, Inc., Austin, Texas 78744, USA; [13]These authors contributed equally.

Abstract

Consumption of high energy Western diet triggers mild adaptive β cell proliferation to compensate for peripheral insulin resistance; however, the underlying molecular mechanism remains unclear. Here we show that the Toll-like receptors TLR2 and TLR4 inhibited the diet-induced replication of β cells in mice and humans. The combined, but not the individual loss of TLR2 and TLR4 increased the replication of β cells, but not that of α cells, leading to enlarged β cell area and

[*]**Corresponding author:** lingq@med.umich.edu.

AUTHOR CONTRIBUTION

Y.J. and S.S. designed and performed most experiments; N.S., L.B.D., H.K., D.A. and M.M. assisted in some experiments; J.S., R.N.K., B.A.C. and M.G. measured TLR expression in human and aged mouse islets; S.A.S. provided helpful discussions and suggestions; C.L. and A.N. provided human islets; Y.X., Y.H., Y.W. and J.O. performed functional analysis of mouse islets; S.K. performed microarray analyses; Y.J. and S.S. wrote the methods and legends; L.Q. designed the experiments, managed the project and wrote the manuscript; everybody edited and approved the manuscript.

COMPETING INTERESTS

The authors declare no competing interests

hyperinsulinemia in diet-induced obesity. Loss of TLR2 and TLR4 increased the nuclear abundance of the cell cycle regulators cyclin D2 and Cdk4 in a manner dependent on the signaling mediator Erk. These data reveal a regulatory mechanism controlling the proliferation of β cells in diet-induced obesity and suggest that selective targeting of the TLR2-TLR4 pathways may reverse β cell failure in diabetic patients.

Keywords

β cell replication; high-fat diet; parabiosis; islet transplantation; mouse models; human islets; Erk; Ccnd2; CDK4; senescence

β cell replacement and regeneration therapies are promising approaches to the treatment of insulin-dependent type 1 diabetes (T1D) and type 2 diabetes (T2D). In rodents and humans, β cells in the pancreas are maintained by neogenesis of β cells from ductal precursor cells and the replication of preexisting β cells[1, 2, 3]. Neogenesis takes place mostly during fetal and neonatal life, and β cell proliferation rates decline dramatically with age. Mitotic replication of β cells, also known as β cell self-renewal, compensates for increased metabolic demands in adults[3, 4, 5, 6, 7, 8]. Western diet or high fat diet triggers mild β cell proliferation and islet mass expansion[9, 10, 11, 12]; however, the mechanism driving this adaptive process remains unclear. In diet-induced obesity, increased metabolic burden increases production of insulin by increasing secretion per β cell and/or by increasing β cell numbers. Insulin and glucose, as well as growth factors and nutrients promote β cell replication, at least in part through the activation of pro-proliferative/pro-survival protein kinases such as Akt and Erk (or Mapk, mitogen-activated protein kinase)[13]. Activation of Akt and Erk-Mapk may induce β cell proliferation by activating cell cycle regulators such as the cyclin D2 and Cdk4 and/or anti-apoptotic factors[7, 14, 15, 16]. This indicates potential negative regulatory mechanism(s) that limit diet-induced β-cell replication, the precise identities of which remain largely unknown.

TLR proteins, a family of conserved cell surface and intracellular proteins, recognize a variety of pathogen-associated molecular patterns and induce innate immune responses. They link innate immunity to adaptive immune responses against all known pathogens such as viruses, fungi, bacteria and protozoa[17, 18, 19]. Among a dozen TLR proteins, TLR4 detects lipopolysaccharides (LPS) found in most gram-negative bacteria, whereas TLR2, in conjunction with TLR1 or TLR6, recognizes lipopeptides (e.g. lipoteichoic acid, LTA) and other components of gram-positive bacteria. It has been reported that TLR2 and TLR4 may mediate nutrient sensing and metabolic regulation in T2D by acting directly or indirectly as sensors for free fatty acids or other lipids in adipose tissue and macrophages[20, 21, 22, 23]. In most reports, loss of either TLR2 or TLR4 in mice fed a high-fat diet (HFD) reduces systemic inflammation in the liver and adipose tissue, and improves insulin sensitivity[24, 25, 26, 27]. However, *Tlr2*$^{-/-}$ and *Tlr4*$^{-/-}$ mice on HFD exhibit mild metabolic phenotypes in term of glucose and insulin sensitivity that may be explained by redundancy in TLR2 and TLR4 function[28]. Here we show that TLR2 and TLR4 regulated β cell proliferation. The combined action of the TLR2 and TLR4-mediated signaling pathways maintained β cell quiescence in an islet-intrinsic manner in mice and humans. Loss of TLR2

and TLR4, but not of each individually, increased β cell proliferation in a HFD-dependent manner.

RESULTS

Regulatory mechanisms counter HFD-induced β cell replication

We first performed immunofluorescent staining and confocal microscopy to quantitate β cell proliferation, marked as $Ki67^+$ and $Insulin^+$ ($Ki67^+Ins^+$) cells, as a function of age in C57BL/6J (B6) male mice on low-fat diet (LFD) or high-fat diet (HFD) with 13% and 60% of calories derived from fat, respectively. Mice were maintained on LFD and for some, were switched to HFD at 6-weeks of age. Percent of $Ki67^+Ins^+$ β cells decreased nearly 50-fold when LFD mice reached 20 weeks of age compared to 4-week-old LFD mice and declined by an additional 4-fold in 45-week-old LFD mice (Fig. 1a). HFD feeding for 39 weeks modestly, but not significantly, increased the percent of $Ki67^+Ins^+$ β cells compared to those age-matched LFD mice at 45 weeks of age (Fig. 1a and Supplementary Fig. 1a). Treatment with the insulin receptor antagonist S961 (to induce systemic insulin resistance[29]) for the last two weeks augmented the percent of $Ki67^+Ins^+$ β cells by 3.5-fold in HFD mice compared to vehicle-treated HFD mice (Fig. 1a and Supplementary Fig. 1a). By contrast, S961 increased the percent of $Ki67^+Ins^+$ β cells by ~120 fold in 45-week-old LFD mice compared to vehicle-treated LFD mice, reaching to a level that was 3-fold higher than in S981-treated HFD mice (Fig. 1a). These observations indicated the existence of a regulatory mechanism that restrained β cell replication in HFD mice.

TLR2 and TLR4 activation blocks β cell proliferation in mice and humans

Compared with those cultured in low (2.8 mM) glucose, treatment of mouse primary islets with high (22.8 mM) glucose for 3 days stimulated the incorporation of the nucleotide analog BrdU in replicating β cells as measured by flow cytometry (Fig. 1b). Treatment with the TLR2- and TLR4-specific agonists, LTA and LPS, for the last 2 days significantly reduced the percent of BrdU+ β cells cultured with 22.8 mM glucose (Fig. 1b). The inhibitory effect of TLR2 and TLR4 agonists on β cell proliferation was blunted in $Tlr2^{-/-}Tlr4^{-/-}$ islets (Fig. 1b). We next investigated the effect of TLR2-TLR4 activation in human islets isolated from three independent donors using the same BrdU incorporation assay (Supplementary Fig. 1b). Activation of TLR2 and TLR4 by LPS + LTA treatment reduced high glucose-induced BrdU incorporation in islets from healthy controls and T2D patients, albeit with large variability among the samples in terms of baseline proliferation (Supplementary Fig. 1c,d). These data suggested that activation of TLR2 and TLR4 may attenuate hyperglycemia-induced β cell proliferation.

TLR2-TLR4 deficiency plus HFD feeding leads to β cell accumulation

Six-week-old $Tlr2^{-/-}Tlr4^{-/-}$ male mice on the B6 background fed a HFD gained body weight comparably to age- and gender- matched non-littermates B6 HFD mice (bred separately) as shown previously[30] (Supplementary Fig. 2a). Serum insulin increased progressively in $Tlr2^{-/-}Tlr4^{-/-}$ HFD mice compared to B6 HFD mice over a 21-week HFD feeding period (Fig. 1c). Histological examination of the pancreas revealed progressively enlarged islet mass and increased abundance of Ins^+ β cells in $Tlr2^{-/-}Tlr4^{-/-}$ HFD mice

compared to age-matched B6 HFD mice over a 51-week HFD feeding period (Fig. 1d and Supplementary Fig. 2b–c). By contrast, number of glucagon$^+$ α cells per islets was unchanged in *Tlr2*$^{-/-}$*Tlr4*$^{-/-}$ HFD mice compared to age-matched B6 HFD mice (Supplementary Fig. 2d–e). After prolonged 51 week-HFD feeding, islets from *Tlr2*$^{-/-}$*Tlr4*$^{-/-}$ HFD mice were visible to the naked eye with a remarkable accumulation of β cells, but not islets from B6 HFD mice (Fig. 1e and Supplementary Fig. 3a). HFD feeding was required for β cell accumulation in *Tlr2*$^{-/-}$*Tlr4*$^{-/-}$ mice because Ins$^+$ β cell area was comparable between *Tlr2*$^{-/-}$*Tlr4*$^{-/-}$ mice and control B6 mice on LFD at 20- and 45-weeks of age (Supplementary Fig. 3b–d).

To exclude possible genetic variability between non-littermate B6 mice and *Tlr2*$^{-/-}$*Tlr4*$^{-/-}$ mice, we crossed the *Tlr2*$^{-/-}$*Tlr4*$^{-/-}$ mice with B6 mice and then interbred the *Tlr2*$^{+/-}$*Tlr4*$^{+/-}$ mice to generate *Tlr2*$^{-/-}$*Tlr4*$^{-/-}$ and *Tlr2*$^{+/+}$*Tlr4*$^{+/+}$ as littermates. In keeping with the above findings, *Tlr2*$^{-/-}$*Tlr4*$^{-/-}$ HFD mice had significantly more Ins$^+$ β cells and elevated insulin in the serum compared to *Tlr2*$^{+/+}$*Tlr4*$^{+/+}$ HFD littermates following 20-week HFD (Fig. 1f–h).

Islet hyperplasia and hyperinsulinemia was linked to insulin resistance in mice with a liver-specific deletion of the insulin receptor[8, 31]. However, 20-week-old *Tlr2*$^{-/-}$*Tlr4*$^{-/-}$ HFD mice exhibited comparable insulin sensitivity to that of age-matched *Tlr2*$^{+/+}$*Tlr4*$^{+/+}$ HFD and B6 HFD mice following 14-week HFD (Fig. 1i–j), suggesting that β cell accumulation in *Tlr2*$^{-/-}$*Tlr4*$^{-/-}$ HFD mice was not due to systemic insulin resistance. Therefore, these data suggested that loss of TLR2 and TLR4 in mice fed a HFD leads to the accumulation of β cells, not triggered by systemic insulin resistance.

TLR2 and TLR4 inhibit β cell proliferation in a HFD-dependent manner

To assess the etiology of β cell accumulation, we next measured β cell proliferation by co-staining pancreatic sections with insulin and proliferation markers such as Ki67 and PCNA. Ki67$^+$Ins$^+$ β cells were barely detectable in 20- and 45-week-old *Tlr2*$^{-/-}$*Tlr4*$^{-/-}$ and control B6 mice on LFD (Fig. 2a). The percent of Ki67$^+$Ins$^+$ β cells in 20- and 45-week-old HFD *Tlr2*$^{-/-}$*Tlr4*$^{-/-}$ mice was increased by 14- and 7-fold, respectively, compared to HFD B6 mice (Fig. 2b,c and Supplementary Fig. 4a). Indeed, Ki67$^+$Ins$^+$ β cells in 20-week-old *Tlr2*$^{-/-}$*Tlr4*$^{-/-}$ mice following 14-week HFD reached 9–10% of the total β cells (Fig. 2b,c). Consistently, expression of PCNA, another proliferation marker, in islets from 35-week-old *Tlr2*$^{-/-}$*Tlr4*$^{-/-}$ HFD mice following 29 weeks of HFD was higher than B6 HFD mice (Fig. 2d). Expression of the mature β cell marker PDX1 on β cells was unchanged in *Tlr2*$^{-/-}$*Tlr4*$^{-/-}$ HFD mice compared to B6 HFD mice following 29 weeks of HFD (Supplementary Fig. 4b), indicating that β cell identity was not affected by TLR deficiency. Moreover, percent of Ki67$^+$Ins$^+$ β cells was consistently 6-fold higher in 26-week-old *Tlr2*$^{-/-}$*Tlr4*$^{-/-}$ HFD mice than *Tlr2*$^{+/+}$*Tlr4*$^{+/+}$ HFD littermates following 20-week HFD (Fig. 2e,f); while few Ki67$^+$Ins$^+$ β cells were detected in 26-week-old *Tlr2*$^{-/-}$*Tlr4*$^{-/-}$ and *Tlr2*$^{+/+}$*Tlr4*$^{+/+}$ littermates on LFD (Supplementary Fig. 4c). Ki67 immunostaining was virtually absent in Glucagon$^+$ α cells in *Tlr2*$^{-/-}$*Tlr4*$^{-/-}$ HFD, *Tlr2*$^{+/+}$*Tlr4*$^{+/+}$ HFD and B6 HFD mice (Fig. 2g and Supplementary Fig. 4d). There was no detectable TUNEL+ β cells in *Tlr2*$^{-/-}$*Tlr4*$^{-/-}$ HFD and B6 HFD mice (Fig. 2h).

Using flow cytometry, we noted that the expression of markers of cellular senescence, including p16^{INK4a} [32] and β-galactosidase on β cells from 9 month old *Tlr2*$^{-/-}$*Tlr4*$^{-/-}$ HFD mice was decreased compared to age-matched B6 mice (Supplementary Fig. 4e,f). Intriguingly, when switched back to LFD for 4 weeks, percent of Ki67^{+} β cells in *Tlr2*$^{-/-}$*Tlr4*$^{-/-}$ HFD mice on 10 week- (short-term) or 32 week- (long-term) HFD dropped by more than 10-fold (Fig. 2i,j and Supplementary Fig. 4g). These data excluded the possibility of oncogenic transformation of β cells or the development of insulinomas in *Tlr2*$^{-/-}$*Tlr4*$^{-/-}$ HFD mice. Hence, loss of TLR2 and TLR4 enhanced the proliferation of β cells in mice on a HFD.

TLR2 and TLR4 blocks nuclear accumulation of the Ccnd2-Cdk4 complex

We next dissected the molecular events underlying the enhanced β cell proliferation in *Tlr2*$^{-/-}$*Tlr4*$^{-/-}$ HFD mice. Ccnd2, a key regulator of cell cycle, enters the nucleus to drive cell cycle progression in β cells[14, 15]. Using immunofluorescent staining, we noted that Ccnd2 was largely nuclear in β cells from *Tlr2*$^{-/-}$*Tlr4*$^{-/-}$ HFD mice vs. largely cytosolic in β cells from B6 HFD mice and *Tlr2*$^{+/+}$*Tlr4*$^{+/+}$ HFD littermates (Fig. 3a, b). Ccnd2 was not detectable in α cells from HFD mice regardless of the genotypes (Supplementary Fig. 5a,b). Nuclear accumulation of Ccnd2 in β cells from *Tlr2*$^{-/-}$*Tlr4*$^{-/-}$ HFD mice was significantly reduced upon switching to LFD for 4 weeks (Fig. 3c) and indeed, Ccnd2 was largely cytosolic in β cells from *Tlr2*$^{-/-}$*Tlr4*$^{-/-}$ LFD mice (Supplementary Fig. 5c). Consistently, Cdk4, which forms a complex with Ccnd2, was highly enriched in the nucleus of β, not α, cells from *Tlr2*$^{-/-}$*Tlr4*$^{-/-}$ HFD mice compared to B6 HFD mice (Fig. 3d and Supplementary Fig. 5d).

We next asked whether the production and secretion of insulin were affected in primary islets from 15-week-old *Tlr2*$^{-/-}$*Tlr4*$^{-/-}$ and B6 mice on HFD for 9 weeks. Cytosolic calcium flux and insulin secretion in response to extracellular stimuli such as glucose and KCl were either enhanced or comparable in islets from *Tlr2*$^{-/-}$*Tlr4*$^{-/-}$ HFD mice compared to those from B6 HFD mice (Fig. 3e). Insulin granules in β cells from *Tlr2*$^{-/-}$*Tlr4*$^{-/-}$ mice on HFD for 51 weeks were similar in size and density relative to those from B6 HFD mice, as assessed by transmission electron microscopy (Fig. 3f), indicating that the *Tlr2*$^{-/-}$*Tlr4*$^{-/-}$ β cells retained normal response to hyperglycemia. Together, these data indicated increased abundance of nuclear Ccnd2-Cdk4 complex and normal secretory function of β cells from *Tlr2*$^{-/-}$*Tlr4*$^{-/-}$ HFD mice.

TLR2 and TLR4 are redundant in controlling β cell replication

To address whether the effects of TLR2 and TLR4 on β cells are redundant or synergistic, we generated and characterized the islet phenotypes of *Tlr2*$^{+/+}$*Tlr4*$^{+/+}$, *Tlr2*$^{-/-}$, *Tlr4*$^{-/-}$ and *Tlr2*$^{-/-}$*Tlr4*$^{-/-}$ littermate mice on the B6 background following 20-week HFD feeding starting at 6 weeks of age. All mice gained weight comparably (Fig. 4a). The islet size and percent of Ins^{+} β cell area per pancreas in the *Tlr2*$^{-/-}$ HFD or *Tlr4*$^{-/-}$ HFD mice were comparable to those in *Tlr2*$^{+/+}$*Tlr4*$^{+/+}$ HFD littermate mice, but significantly lower than those in *Tlr2*$^{-/-}$*Tlr4*$^{-/-}$ HFD littermate mice (Fig. 4b,c). Using immunofluorescent staining, we detected very few Ki67^{+} or nuclear Ccnd2^{+} β cells in islets from HFD *Tlr2*$^{-/-}$ or HFD *Tlr4*$^{-/-}$ mice, unlike those in *Tlr2*$^{-/-}$*Tlr4*$^{-/-}$ HFD littermates (Fig. 4d–f). Activation of TLR2

or TLR4 by LTA or LPS, respectively, in islets from B6 mice *in vitro* reduced BrdU incorporation in Ins^+ β cells to a similar extent as LPS+LTA (Fig. 4g). These data suggested that activation of either TLR2 or TLR4 was sufficient to suppress β cell proliferation in mice on a HFD.

TLR2 and TLR4 regulate islet expansion in an islet-intrinsic manner

β cell proliferation can be controlled locally in a paracrine fashion[33, 34, 35] or systemically by hepatokines in an endocrine fashion[36]. To distinguish between these possibilities we surgically joined $CD45.1^-$ *Tlr2*$^{-/-}$*Tlr4*$^{-/-}$ and $CD45.1^+$ B6 mice at 8 weeks of age and following a 3-week recovery period, placed them on a HFD for 14 weeks. The B6-*Tlr2*$^{-/-}$*Tlr4*$^{-/-}$ parabiotic pairs exhibited similar weight gain on HFD as control *Tlr2*$^{-/-}$*Tlr4*$^{-/-}$- *Tlr2*$^{-/-}$*Tlr4*$^{-/-}$ and B6-B6 pairs on HFD (Fig. 5a). Flow cytometry indicated the equilibration of $CD4^+$ T cells, $CD8^+$ T cells and $CD19^+$ B cells in the blood of the parabiotic pairs 3 weeks post-surgery (Fig. 5b). The In^+ β cell area did not change in the *Tlr2*$^{-/-}$*Tlr4*$^{-/-}$ or the B6 partners of the B6-*Tlr2*$^{-/-}$*Tlr4*$^{-/-}$ pairs compared to those in *Tlr2*$^{-/-}$*Tlr4*$^{-/-}$-*Tlr2*$^{-/-}$*Tlr4*$^{-/-}$ and B6-B6 pairs, respectively (Fig. 5c), excluding a major effect of host-derived soluble factor(s) in the islet expansion of HFD *Tlr2*$^{-/-}$*Tlr4*$^{-/-}$ mice.

Next we addressed whether TLR2 and TLR4 were expressed in islets. As determined by RT-PCR, *Tlr2* and *Tlr4* mRNA were expressed in primary islets from age-matched B6 mice on LFD or HFD for 7 months starting at the age of 6 weeks (Fig. 5d). While expression of *Tlr4* mRNA decreased with age, *Tlr2* expression remained unchanged in islets from 2–12 month-old B6 mice on LFD (Supplementary Fig. 6a). In humans, *TLR2*, but not *TLR4* mRNA, was significantly increased in islets isolated from T2D patients as compared to the healthy controls (Fig. 5e).

To test whether the role of TLR2 and TLR4 in β cells was islet-intrinsic we transplanted similar size primary islets isolated from LFD B6 and *Tlr2*$^{-/-}$*Tlr4*$^{-/-}$ mice (Fig. 6a) under the capsules of the left (B6 islets) and right (*Tlr2*$^{-/-}$*Tlr4*$^{-/-}$ islets) kidneys of 10-week-old recipient B6 or *Tlr2*$^{-/-}$*Tlr4*$^{-/-}$ mice treated with a single high-dose of diabetogenic agent streptozotocin (STZ) to induce diabetes. After a 4-week recovery period, islet recipients were switched to a HFD diet (Supplementary Fig. 6b) and steadily gained weight for a total of 14 weeks (Fig. 6b). Within a week post-transplantation, STZ-treated diabetic recipients exhibited improved glycemia (Fig. 6c), indicative of a successful islet transplantation. After 14 weeks on a HFD, *Tlr2*$^{-/-}$*Tlr4*$^{-/-}$ islet grafts grew much larger than B6 islet grafts in either B6 or *Tlr2*$^{-/-}$*Tlr4*$^{-/-}$ recipients (Supplementary Fig. 6c). Histological analyses indicated significantly larger islet area and more Ins^+ cells in the *Tlr2*$^{-/-}$*Tlr4*$^{-/-}$ islet grafts compared to the B6 islet grafts (Fig. 6d). Confocal microscopy revealed elevated numbers of $Ki67^+Ins^+$ β cells and more nuclear $Ccnd2^+$ β cells in *Tlr2*$^{-/-}$*Tlr4*$^{-/-}$ islet grafts compared to B6 islet grafts (Fig. 6e,f). Blood vascularization of the islet grafts was comparable between B6 and *Tlr2*$^{-/-}$*Tlr4*$^{-/-}$ islets (Supplementary Fig. 6d), excluding a possible contribution of vascularization in differential islet expansion[37]. Together, these experiments argued against a role of circulating host-derived factors in islet expansion of *Tlr2*$^{-/-}$*Tlr4*$^{-/-}$ HFD mice and suggested that TLR2 and TLR4 deficiency affected HFD-induced β cell replication in an islet-intrinsic manner.

TLR2-TLR4 regulate HFD-induced β cell proliferation via Erk

We next explored the molecular link between TLR2-TLR4 deficiency and HFD-induced β cell proliferation. We performed unbiased global transcriptional profiling of islets from B6 and *Tlr2*$^{-/-}$*Tlr4*$^{-/-}$ mice following 7-month HFD. GSEA pathway analysis revealed a significant increase of pathways linked to cell cycle progression and replication in islets from HFD *Tlr2*$^{-/-}$*Tlr4*$^{-/-}$ mice (Supplementary Fig. 7a). We observed the differential regulation of ~101 genes whose levels were altered by more than 2.0-fold in islets from HFD *Tlr2*$^{-/-}$*Tlr4*$^{-/-}$ mice compared to those from HFD B6 mice (False discovery rate, FDR q<0.05), including *Reg2* (Fig. 7a and Supplementary Fig. 7b). *Reg2* is a gene highly induced in islet regeneration[38] and required for compensatory islet proliferation and expansion in obesity and aging[39]. Similar results were obtained in islets following a short-term 5 week HFD (Fig. 7a and Supplementary Fig. 7c,d). The induction of *Reg2* mRNA in *Tlr2*$^{-/-}$*Tlr4*$^{-/-}$ islets from HFD mice suggested a unique signature for the highly proliferative β cell population in the *Tlr2*$^{-/-}$*Tlr4*$^{-/-}$ HFD mice compared to B6 HFD mice.

We next analyzed the status of various signaling pathways known to be implicated in β cell proliferation. Phosphorylation of Erk1/2 proteins was increased by 2–3 fold in islets from HFD *Tlr2*$^{-/-}$*Tlr4*$^{-/-}$ mice compared to HFD B6 mice (Fig. 7b), while phosphorylation of other kinases, including Akt, AMPK, Jnk, IκB and p-NF-κB was unchanged (Fig. 7c). In line with elevated Erk activation, the upstream kinases MEK1/2 were hyperphosphorylated in islets from HFD *Tlr2*$^{-/-}$*Tlr4*$^{-/-}$ mice compared to HFD B6 mice (Fig. 7b). p16^{INK4a}, a known downstream target of the Erk pathway in β cells[40], was downregulated in islets from HFD *Tlr2*$^{-/-}$*Tlr4*$^{-/-}$ mice compared to HFD B6 mice (Supplementary Fig. 4e). LPS+LTA treatment suppressed high glucose-induced Erk1/2 phosphorylation in islets from B6 LFD mice, which was blunted in islets from *Tlr2*$^{-/-}$*Tlr4*$^{-/-}$ LFD mice (Fig. 7e, f). Moreover, LPS +LTA treatment blocked the nuclear accumulation of Ccnd2 and Cdk4 proteins induced by high glucose in primary islets from B6 LFD mice *in vitro* (Fig. 7g and Supplementary Fig. 8a–b). Treatment of B6 islets with either LPS or LTA suppressed phosphorylation of Erk (Supplementary Fig. 8c), suggesting the redundant function of TLR2 and TLR4 in blocking Erk phosphorylation. Treatment with LPS+LTA in macrophages had the opposite effect on phosphorylation of Erk (Supplementary Fig. 8d), pointing to a specific effect of TLR2-TLR4 activation in Erk activation in islets.

Lastly, oral administration of the small-molecule MEK inhibitor MEK162, an FDA-approved drug known as Binimetinib, blocked ERK activation (Supplementary Fig. 8e), reduced the number of Ki67^{+}Ins^{+} β cells (Fig. 7h and Supplementary Fig. 8f) and the abundance of nuclear Ccnd2 in β cells (Fig. 7i) in 14-week-old *Tlr2*$^{-/-}$*Tlr4*$^{-/-}$ mice on HFD for 8 weeks. Taken together, these data suggested that TLR2-TLR4 signaling pathways in HFD mice attenuated β cell proliferation in a MEK-Erk-dependent manner.

DISCUSSION

Here we describe a regulatory mechanism underlying the diet-induced β cell proliferation. While activation of TLR2 and TLR4 in vitro blocks high glucose-induced β cell proliferation in primary mouse and human islets, the loss of TLR2 and TLR4, together but not individually, increases β cell proliferation and attenuates β cell senescence. This leads to

massive β cell accumulation in a mouse model of diet-induced obesity. We further demonstrate that the effect of TLR2 and TLR4 on islet β cell accumulation in HFD mice is islet autonomous and depends on HFD feeding.

Our results suggest that β cell proliferation was regulated by both positive and negative signals in diet-induced obesity, with positive signals provided by β-cell trophic factors such as nutrients, growth factors and/or insulin resistance being opposed by negative signals exerted by TLR2 and TLR4. Our data show that, during chronic HFD feeding, TLR2 and TLR4-mediated signaling pathways downregulate the activation of MEK-Erk and reduce the nuclear entry of the Ccnd2-Cdk4 complex, thereby limiting β cell proliferation. When TLR2 and TLR4 are simultaneously disrupted, β cell replication was enhanced by the positive signals associated with HFD feeding, but continued to maintain their characteristic features and functions. These interpretations are supported by a report showing that the prostaglandin E2 receptor, EP3, acts as a negative regulator of β cell proliferation in mouse and human under conditions of stress such as hyperglycemia and insulin resistance[41].

Our data point to an islet-intrinsic role for TLR2-TLR4 signaling. β cell proliferation is known to be responsive to manipulation and enhanced by genetic or pharmacological means[13, 42]. Unlike β cell adenomas in mice with overexpression of Cdk4[32] or loss of the tumor suppressor gene Menin[43], in which islet expansion is constitutive, islet expansion in the *Tlr2*$^{-/-}$*Tlr4*$^{-/-}$ mice is reversible and is dependent on HFD. The secretory function of *Tlr2*$^{-/-}$*Tlr4*$^{-/-}$ β cells is not compromised, as they exhibit a normal response to various stimuli (e.g. glucose and KCl), suggesting hyperinsulinemia in the *Tlr2*$^{-/-}$*Tlr4*$^{-/-}$ mice was not due to unregulated and constitutive insulin secretion, but rather to compensatory β cell accumulation. Moreover, *Tlr2*$^{-/-}$*Tlr4*$^{-/-}$ mice are normoglycemic on HFD, and did not develop hypoglycemia, which is often associated with unregulated hyperinsulinemia. Finally, although we detected ~10% of β cells proliferating in the *Tlr2*$^{-/-}$*Tlr4*$^{-/-}$ mice on a HFD, this was likely an underestimate, because the data were obtained from a single point to provide a snapshot of proliferating cells.

The finding that islet expansion in *Tlr2*$^{-/-}$*Tlr4*$^{-/-}$ mice occurs most significantly in the context of diet-induced obesity is consistent with the notion that diet-induced obesity is associated with the activation of TLR2 and TLR4 signaling pathways[23]. Previous studies have shown that obesity-associated insulin resistance may enhance β cell numbers through non-β-cell-autonomous mechanisms. One suggested mechanism involves Erk activation in the liver in diabetes, leading to β cell proliferation in a neuronal signal-dependent manner, although the molecular nature of the neuronal signal remains unclear[44]. Another proposed mechanism involves the disruption of insulin signaling in the liver[31], which leads to the compensatory proliferation of β cell stimulated by the liver-derived factor serpinB1[36]. However, these mechanisms do not appear to explain the proliferation of β cells in the HFD *Tlr2*$^{-/-}$*Tlr4*$^{-/-}$ mice, because these are not more insulin resistant following long-term HFD compared to wild-type mice on a HFD. Moreover, islet transplantation and parabiosis experiments exclude a possible role for circulating or neuronal factors or other non-islet cells, including hepatocytes and neurons, in this process. Purported activation of TLR2 and/or TLR4 by gut microbiota derivatives and/or fatty acids may represent a mechanism for the limited β cell proliferation in response to HFD[23]. In this context, further studies are

warranted to explore whether TLR agonists, such as free fatty acids, other lipids and bacterial toxins function as upstream ligands of TLRs in islets.

TLR2 and TLR4 in immune cells have the ability to sense molecular patterns from invading pathogens and to bridge the innate and adaptive immune responses. Our results extend the signaling through TLR2 and TLR4 to islet β cell replication and islet expansion. It is possible that TLR2 and TLR4 in islets may integrate inflammatory signals in diet-induced obesity to attenuate adaptive changes that govern β cell replication, a previously underappreciated interplay between the metabolic and innate immune systems[23]. β cell proliferation may be more tightly linked to systemic inflammatory status than previously anticipated. Future studies will address whether blocking TLR2 and TLR4 signaling, using either small molecule antagonists, genetic editing or bi-potent TLR2-TLR4 antibodies, may enhance human β cell replication. Delineation of the immediate downstream pathways of TLR2-TLR4 in β cells may also help guide future efforts to target them as a promising strategy to expand β cells in diabetes.

METHODS

Mice

Tlr2$^{-/-}$*Tlr4*$^{-/-}$ mice were originally generated by S. Akira (Osaka University) and provided to us by L. Hajjar (University of Washington) and David Russell (Cornell University). These *Tlr2*$^{-/-}$*Tlr4*$^{-/-}$ mice have been backcrossed to the B6 background for 6 generations as previously described[30, 45]. Non-littermate B6 wild-type mice (#000664) were purchased from the Jackson Laboratory and bred in our facility. To generate *Tlr2*$^{+/+}$*Tlr4*$^{+/+}$ and *Tlr2*$^{-/-}$*Tlr4*$^{-/-}$ as littermates, we crossed *Tlr2*$^{-/-}$*Tlr4*$^{-/-}$ mice with B6 mice to generate *Tlr2*$^{+/-}$*Tlr4*$^{+/-}$ mice, which then intercrossed to generate *Tlr2*$^{-/-}$, *Tlr4*$^{-/-}$, *Tlr2*$^{-/-}$*Tlr4*$^{-/-}$ and *Tlr2*$^{+/+}$*Tlr4*$^{+/+}$ wild-type littermates. All mice were bred, reared and housed in our specific pathogen-free facility at the University of Michigan Medical School. Age- and gender-matched mice were used as cohorts in the studies. Mice were fed a LFD composed of 13% (calories) fat, 67% carbohydrate, and 20% protein from Harlan Teklad (#2914), or a HFD, starting at 6 weeks of age, composed of 60% fat, 20% carbohydrate, and 20% protein from Research Diets Inc. (D12492) for up to a year. The fatty acid composition of these diets has been described previously[46]. All animals were sacrificed by cervical dislocation and tissues were immediately harvested. Frozen tissues were stored at −80°C. All animal procedures were approved by and done in accordance with IACUC at Cornell University (#2007–0051) and the University of Michigan Medical School (#PRO00006888).

Human islet studies:

(a) Donor info for Q-PCR analysis of TLR expression in islets from the Joslin Diabetes Center (R.K.):

Gender: Ethnicity/Race Age BMI Diabetic donor status

Male: Hispanic/Latino 49 31.3 Non-DM

Female: White 52 31.4 Non-DM

Female: Hispanic/Latino 24 19.5 Non-DM

Male: Hispanic/Latino 58 31.2 Non-MD

Female: White 36 42.7 Non-DM

Male: Caucasian 49 28.2 T2D

Male: Unknown 53 31.0 T2D

Male: Caucasian 48 35.8 T2D

Male: Asian 49 23.9 T2D

Male: Asian 49 23.9 T2D

Total RNA was extracted using RNeasy Kit (Qiagen). cDNAs were synthesized using a High-Capacity cDNA RT Kit (ABI). Q-RT PCR analysis of TLR expression was performed with SYBR Green (Bio-Rad) using ABI 7900HT.

All studies involving human islets at the Joslin Diabetes Center were undertaken using samples obtained from the Integrated Islet Distribution Program (IIDP) funded by the NIH. All islet samples were de-identified and no data was obtained that included individually identifiable information through interventions or interactions with living individuals. This research practice is consistent with the Human Subject Research Determination by the Committee of Human Studies of the Joslin Diabetes Center.

(b) Donor info for flow cytometric analysis of β cell proliferation in islets from the Integrated Islet Distribution Program (IIDP) at UPENN (C.L. and A.N.).

Gender: Ethnicity/Race Age BMI Diabetic donor status

Female (Donor 1): Hispanic 24 32.2 Non-DM

Male (Donor 2): Caucasian 46 19.13 Non-DM

Male (Donor 3): Caucasian 47 32.2 T2D

We at UPENN received all pancreatic organs from the Organ Procurement Organizations (OPOs) Gift of Life program. All organ donations have been consented for both clinical and research use. We followed the Clinical Islet Transplantation (CIT) SOP protocols for all islet isolations. The islets were distributed per the Integrated Islet Distribution Program (IIDP) protocols. High-quality islet preparation with over 80–90 percent of viability was sent to the Qi laboratory at the University of Michigan Medical School. Upon arrival, islets were treated as described below.

Islet transplantation under kidney capsules of diabetic mice

Islet kidney transplantation was performed as described previously[47, 48]. Recipient B6 or *Tlr2*$^{-/-}$ *Tlr4*$^{-/-}$ mice at the age of 6–10 weeks were injected with a single high-dose of

streptozotocin (STZ, Sigma) at 150 mg/kg body weight. Mice with ad libitum blood glucose higher than 300 mg/dl were defined as diabetic and used as recipients. On the day of surgery, mice were anesthetized by isoflurane inhalation. After preparation of surgical-area skin, a 2 cm incision was made through the dermis right above the kidney. A small incision was further made on the peritoneal wall to expose the kidney. Using a 27-gauge needle, a small nick was made on the kidney capsule. Collected islets were in advance transferred and sedimented in a flexible PE50 tubing. The beveled end of the islets-containing PE50 tubing was carefully placed under the capsule, and the tubing was moved around gently to make a small pouch under kidney capsule. Islets were slowly delivered from the tubing into the subscapular pouch by gentle depressing the plunger of a 25 μl Hamilton syringe that was connected to the other end of the tubing. 100 primary islets isolated from donor B6 and *Tlr2*$^{-/-}$ *Tlr4*$^{-/-}$ mice were implanted under the capsule of either left or right kidney of the recipient. The nick on the kidney was cauterized with low heat. The kidney was placed back into the cavity and the peritoneum and skin were sutured. Ketoprofen were given preemptively (20–30 min prior to surgery) at the rate of 2.5–5 mg/kg subcutaneously and were continued once daily for next 2–3 days. After a 4-week recovery, mice were given HFD for 14 weeks, and kidneys were collected for histological analysis after euthanasia.

Parabiosis

Parabiosis was performed as previously described[49]. Female mice in the same cage were anesthetized using an isoflurane vaporizer and then shaved thoroughly starting at 1 cm above the elbow to 1 cm below the knee on the side to be connected during parabiosis. Then a longitudinal skin incision was performed at the shaved side and the skin was gently detached from the subcutaneous fascia to create about 0.5 cm of free skin. Mice were then joined by attaching the olecranon and the knee together and the skin was sutured ventrally from the elbow towards the knee followed by continuous dorsal stitches. Three weeks after the surgery, parabiotic pairs were fed on HFD and monitored for body weight and blood glucose levels. After 14-weeks of HFD feeding, mice were sacrificed for histological examination of the pancreas. To test blood chimerism, CD45.1^{+} B6 mice (B6.SJL-*Ptprc*^{a} *Pepc*^{b}/BoyJ, Jackson Laboratory) and CD45.1^{-} *Tlr2*$^{-/-}$ *Tlr4*$^{-/-}$ mice were surgically joined, and the percent of CD45.1^{+}/CD45.1^{-} hematopoietic cells in the blood of paired mice were determined by flow cytometry.

Drug treatment *in vivo*

For S961 studies, 45-week-old mice under a LFD or HFD were anesthetized and subcutaneously implanted with osmotic pumps (ALZET) filled with insulin receptor antagonist S961[36] or vehicle PBS. Mice were infused with S961 at the dose of 10 nmoles/week for 2 weeks, followed by euthanasia and histological analysis of islets. For MEK162 studies, *Tlr2*$^{-/-}$ *Tlr4*$^{-/-}$ mice on HFD for 8 weeks were orally gavaged with MEK162 (20 mg/kg body weight, LC laboratories) or vehicle, twice daily for 2 days, followed by euthanization and histological analysis.

Purification of primary mouse islets

The duodenal opening of the bile duct was clamped with a hemostat, and the bile duct was cannulated and perfused with 2 ml Liberase TL Research Grade (0.3 mg/ml, Roche) in

RPMI 1640 medium (Invitrogen). The perfused pancreas was removed and incubated at 37°C for 30 min, after which the digestion was stopped by adding 20 ml of cold RPMI1640 medium containing 10% serum (FISHER). Digested pancreas was further dissociated mechanically by vigorous shaking. After two washes in RPMI1640 medium, the digested tissues were filtered through a 450 μm nylon mesh and resuspended in a Histopaque 1077 (Sigma)/ RPMI1640 medium and centrifuged at 2400 RPM for 20 min. The islets were collected from the interface between the medium and Histopaque and resuspended in RPMI1640 medium containing 10% serum. Islets were washed three times and hand-picked under a light microscope. The islets were cultured overnight in RPMI1640 medium containing 10% serum for analyses.

Human islets

Human islets were received from the accredited Human Islet Resource Center at the University of Pennsylvania. The pancreata were obtained from the donors through the local organ procurement organization. The islets were isolated following the guidelines of Clinical Islet Transplantation (CIT) consortium protocol[50]. Briefly, the pancreas was digested following intraductal injection of Collagenase & Neutral Protease (Serva) in Hanks' balanced salt solution. Liberated islets were then purified on continuous density gradients (Cellgro/Mediatech) using the COBE 2991 centrifuge and cultured in CIT culture media and kept in a humidified 5% CO_2 incubator.

Insulin tolerance tests

For insulin tolerance test (ITT), mice were fasted for 4–6 h followed by injection of insulin (Sigma) at 40 μg/kg body weight. Blood glucose was monitored using TRUEresult Glucometer (Nipro Diagnostics) at indicated time points.

Confocal immunofluorescent and immunohistochemistry staining

Pancreas was fixed in 4% paraformaldehyde, embedded in paraffin, and sectioned by Histology Core Facility at Cornell and University of Michigan. For Hematoxylin/eosin staining, ten-micrometer-thick paraffin sections were stained and imaged using Aperio Scanscope. For immunostaining, paraffin-embedded sections were rehydrated with sequential wash in xylene, 100%, 95%, 75% ethanol and water and boiled in 1 mM EDTA for antigen retrieval. Subsequently, sections were blocked using 5% donkey serum and incubated at 4 °C overnight with primary antibodies: Anti-insulin (Abcam ab7842 or Linco 4011, 1:200), glucagon (Sigma K79bB10, 1:1000), Ki-67 (Abcam ab15580, 1:50), Pcna (Santa Cruz sc-56, 1:100), CD31 (Santa Cruz sc-1506, 1:100), Pdx1 (Cell Signaling D59H3, 1:100), Cdk4 (Santa Cruz sc-260, 1:100) and Ccnd2 (Santa Cruz sc-593, 1:100). Following day, slides were washed and incubated with conjugated secondary antibodies and mounted on slides with prolong gold antifade/ DAPI for nuclear staining. Fluorescence Images were captured under a Nikon A1 confocal microscope at Brehm Diabetes Research Center Imaging Facility at University of Michigan. For horseradish peroxidase enzyme (HRP) staining, slides were stained with Histostain kit and DAB substrate from Invitrogen.

Image quantitation

For quantification of β cell area, six independent pancreatic tissue sections from 3–4 mice were randomly selected. Total Ins^+ and total pancreas area was measured using the Aperio Imagescope and ImageJ, from which percentage of Ins^+area was calculated. For quantitation of β cell proliferation, cytoplasmic insulin and nuclear $Ki67^+Ins^+$ cells were counted as proliferating β cells. Percentage of proliferating β cells were calculated by dividing the number of $Ki67^+Ins^+$ cells by total Ins^+ cells in each islet.

Transmission electron microscopy (TEM)

Pancreatic tissues were collected from mice after 51-week HFD feeding and immediately sliced into 1- to 2-mm^3 pieces and fixed, stained, dehydrated, and embedded in Poly/bed 812 (Polysciences). Embedded samples were cut with Leica Ultracut Ultramicrotome system and images were taken using JEM-1400 TEM on a fee-for-service basis at the Electron Microscopy and Histology Core Facility at Weill Cornell Medical College.

Islet imaging and perifusion

All imaging and perifusion experiments were performed in University of Virginia and conducted according to previously described methods[51, 52]. In brief, islets were incubated in Krebs Ringer buffer (KRB) containing 2 mM glucose, 5 μM Fura-2/AM (Molecular Probes, CA) and 2.5 μM Rhodamine 123 (Sigma, MO) for 30 mins. The islets were then loaded into the temperature equilibrated microfluidic device mounted on an inverted epifluorescence microscope (Leica DMI 4000B, location). The KRB containing 14 mM glucose (20 min) or 30 mM KCl (15 min) was then administered to the islets. Dual-wavelength Fura-2/AM was excited at 340 and 380 nm and fluorescent emission was detected at 510 nm. These images were collected with a CCD (Retiga-SRV, Fast 1394, QImaging). Simple PCI software (Hamamatsu Corp. location) was used for image acquisition and analysis. Intracellular Ca^{2+} was expressed as a ratio of fluorescent emission intensity F340 / F38. All fluorescence signals were expressed as “change-in-percentage” after being normalized against basal intensity levels established before stimulation. Perifusate samples were collected every 2 mins at the outlet at flow rate of 250 μl/min for insulin analysis using Mercodia Rodent Insulin ELISA kit (Uppsala, Sweden).

In vitro islet treatment

Islets were cultured in RPMI 1640 culture medium (10% FCS, 10 mM HEPES, 1 mM sodium pyruvate) overnight after isolation. Islets were then cultured in medium containing 2.8 mM glucose (Low Glucose), 22.8 mM glucose (High Glucose), or stimulated with a combination of LPS (Sigma, 20 μg/ml) and lipoteichoic acid (LTA, Sigma, 2 μg/ml) in 22.8 mM glucose medium for 48 hr. Islets were snap-frozen for mRNA or protein extraction.

INS-1 cell line

Rat β cell line Ins-1 cells were obtained from ThermoFisher and authenticated by morphology, insulin expression and insulin secretion. Cells were cultured in RPMI 1640 culture medium (10% FCS, 10 mM HEPES, 1 mM sodium pyruvate). Ins-1 cells were treated with MEK162 or vehicle for 1 hr and snap-frozen for protein extraction.

Preparation of primary macrophages

Peritoneal macrophages were obtained 4 days after intraperitoneal injection of 2 ml aged 4% brewed thioglycollate broth (VWR 90000–294). Mice were euthanized and macrophages were collected by injection of PBS into the peritoneal cavity and flush. The peritoneal exudate cells were centrifuged at ~1,000 rpm for 10 min and treated with red blood cells lyses buffer. Macrophages were suspended in culture medium and plated in 6-well plate. Macrophages were then cultured in medium containing 2.8 mM glucose (Low Glucose), 22.8 mM glucose (High Glucose), or stimulated with a combination of LPS (200 ng/ml) and lipoteichoic acid (LTA, 1 μg/ml) in 22.8 mM glucose medium, for 24 hr. Cells were snap-frozen for protein extraction.

Flow cytometric/confocal analysis of β cell proliferation and senescence

Mouse and human islets were dissociated with Trypsin-EDTA (Thermofisher, 0.5%) and cultured in 96 well plate with RPMI 1640 medium containing 2.8 mM (low glucose) or 22.8 mM glucose (high glucose), with or without 20 μg/ml LPS and/or 2 μg/ml LTA, for 72 hr. Medium was changed every 24 hr. BrdU (10 μM) was added for the last 48 hr. Cells were collected and fixed in 4% PFA at 4 °C for 15 min. The samples were permeabilized with a BD Cytofix/Cytoperm fixation/permeabilization kit according to the manufacturer's protocol, followed by digestion with DNase I (Roche, 50 U/ml in 4.2 mM $MgCl_2$ and 150 mM NaCl) at room temperature for 30 min. The rest of the procedures were performed as the regular flow cytometric analysis using anti-BrdU-PE (MOPC-21, BD Biosciences) and anti-insulin antibody (Abcam). For analysis of $p16^{INK4a}$ expression, permeabilized cells were stained with anti-insulin and anti-p16 antibody (Santa Cruz 377412, 1:100). For analysis of cell senescence, dissociated β cells were cultured in RPMI 1640 medium containing 33 μM C_{12}FDG (ThermoFisher) at 37 °C for 1 hour. Samples were analyzed using BD LSR cell analyzer at the Vision Research Core Facility at the University of Michigan Medical School. Data were analyzed using the FACSDiva v6.2 software (BD Biosciences) and Flowjo (Flowjo.com). For analysis of Ccnd2 and CDK4 in β cell in vitro, islets were dissociated and cultured on chamber slide (Nunc™ Lab-tek™) with RPMI 1640 medium containing 2.8 mM (low glucose) or 23.8 mM glucose (high glucose), with or without 20 μg/ml LPS and 2 μg/ml LTA, for 72 hr. Cells were fixed and proceeded for immunostaining and confocal imaging as described above.

Flow cytometric analysis of parabiosis

Flow cytometric analysis of peripheral blood cells of parabionts were performed as described before[30, 53]. The RBCs in the blood were lysed and resuspended in cold PBS containing 5% FBS and 1% penicillin/streptomycin. The cell suspension was stained with 1:100 or 1:200 fluorochrome- or biotin-conjugated antibodies against CD4 (GK1.5), CD8 (Lyt2), CD45.1 (Ly-5.1), CD19 (6D5), avidin-PerCP or isotype control antibodies (BioLegend or BD Biosciences). The samples were analyzed by BD LSR cell and the data were analyzed using the CellQuest software (BD Biosciences) and Flowjo (Flowjo.com).

Insulin and multiplex ELISA analyses

Serum insulin levels were measured following a 4 hour fast using ultrasensitive mouse/rat insulin ELISA kit (Crystal Chem) per supplier's instruction. For multiplex analysis, serum samples were collected from indicated mouse cohorts following a 4-hr fast and levels of various hormones were analyzed by Bio-Plex Pro™ Mouse Diabetes Panel 8-Plex (Cat. #171-F7001M) per manufacturer's instruction.

Western blot and antibodies

Preparation of whole cell lysates and Western blots were performed as previously described[54]. Phosphatase Inhibitor (LC laboratories) was added to inhibit phosphatase activity. Antibodies used in this study were: HSP90 (H-114, 1:6,000) and JNK1/2 (sc-571, 1:2,000) from Santa Cruz; p-Thr202/Tyr204 ERK1/2 (4370, 1:2,000), ERK1/2 (9102, 1:2,000), p-Ser217/221 MEK1/2 (9121, 1:1,000), MEK1/2 (4694, 1:1,000), p-Thr183/Tyr185 JNK1/2 (9255S, 1:2,000,), p-Ser473 AKT (9271S, 1:2,000), AKT (9272, 1:2,000), IκBα (9242, 1:2,000), p-Ser536 NFκB p65 (3033, 1:1,000), p-Thr172 AMPKα (2535, 1:2,000) and AMPKα (2532, 1:2,000) from Cell Signaling. Band density was quantitated using the Image Lab software on the ChemiDOC XRS+ system (Bio-Rad). Protein levels were normalized to HSP90 and the phosphorylated forms were normalized to phosphorylation-independent levels of the same protein. Data are presented as mean ± SEM unless otherwise specified. Uncropped blots are shown in Supplementary Fig. 9–11.

TUNEL staining.

TUNEL staining was performed as previously described[2]. Briefly, paraffin-embedded pancreatic sections were rehydrated, treated with protease K, and stained for 1 hour at 37°C using the in Situ Death Detection TUNEL Kit (Roche 11684795910). For positive control, slides were treated with DNase I (Roche) for 30 minutes at room temperature. Fluorescence Images were captured under a Nikon A1 confocal microscope at Brehm Diabetes Research Center Imaging Facility at the University of Michigan.

RNA extraction, reverse transcription (RT) and quantitative PCR (Q-PCR)

RNA extraction from cells and animal tissues, reverse transcription and Q-PCR analyses were performed as previously described[55]. Q-PCR data were collected using Roche LightCycler 480 and gene expression was normalized to ribosomal *l32* gene for each sample. Q-PCR primers used for mouse and human genes:

hTLR2 (TGATGCTGCCATTCTCATTC, CGCAGCTCTCAGATTTACCC)

hTLR4 (GGAGGAAGGGAGAAATGAGG, CACCTCCAAAAGCTTCCTTG)

mTlr2 (GCTGGAGGACTCCTAGGCT, GTCAGAAGGAAACAGTCCGC)

mTlr4 (GCTTTCACCTCTGCCTTCAC, GAAACTGCCATGTTTGAGCA)

mL32 (GAGCAACAAGAAAACCAAGCA, TGCACACAAGCCATCTACTCA)

mMtp (TACCCGTTCTTGGTCTGCAT, TCTGGCTGAGGTGGGAATAC)

mIns2 (GAAGTGGAGGACCCACAAGT, AGTGCCAAGGTCTGAAGGTC)

The Q-PCR conditions were: 94 °C for 5 min, [94 °C for 15 sec, 58 °C for 15 sec and 72 °C for 30 sec] (40 cycles), followed by dissociation curve analysis. The RT-PCR conditions are: 94 °C for 5 min, [94 °C for 15 sec, 58 °C for 15 sec and 72 °C for 30 sec] 30 to 40 cycles according to individual template, followed by 70 °C for 10 min.

Microarray

Islets were collected from mice on a HFD for 5 weeks or 7 months and snap-frozen in liquid nitrogen. RNA was extracted as described above. RNA quality and concentration were determined using the RNA 6000 Nano kit on an Agilent 2100 bioanalyser. The cDNA microarray of islets RNA was performed as previously described[54]. Gene Expression Omnibus (GEO) accession number for the microarray is GSE101392.

Power analysis of the animal size

Based on sample size formula of the power analysis, $N=8(CV)^2[1+(1-PC)^2]/(PC)^2$, to reach the error = 0.05, Power = 0.80, percentage change in means (PC) = 20%, co-efficient of variation (CV) = 10 ~ 15% (varies between the experiments), 4–6 mice per group are the minimal number of mice to obtain statistical significance. Together with our prior experience, we routinely used a total of 4–6 mice in each study to ensure adequate power. Mice in each group were randomly chosen based on the age, genotype and gender.

Statistical analysis

Results were expressed as mean ± SEM. We performed the normality Kolmogorov-Smirnov test using the Prism software first, then parametric tests were performed on the experimental groups. Comparisons between groups were made by unpaired two-tailed Student's *t* test (two groups) and one-way ANOVA with Newman-Keuls post-test (multiple groups). All experiments were repeated at least twice or performed with independent samples.

Life Sciences Reporting Summary.

Further information on research design is available in the Nature Research Reporting Summary linked to this article.

DATA AVAILABILITY

Microarray data supporting the findings of this study have been deposited into the Gene Expression Omnibus (GEO) with accession number GSE101392. All other relevant data are available from the corresponding author upon request.

Supplementary Material

Refer to Web version on PubMed Central for supplementary material.

ACKNOWLEDGEMENTS

We thank L. Hajjar and D. Russell for sharing reagents, Histology and Vision Research Core Facilities at University of Michigan Medical School and TEM core facility at Weill Cornell Medical College for their assistance, and P. Arvan and R. B. Reinert, G. H. Kim, X. Shu as well as other members of the Qi/Arvan labs and islet club at University of Michigan Diabetes Center for comments and technical assistance. The Histology Core at the University of Michigan Medical School was supported by NCI of the NIH under award P30CA046592. This work was supported by NIH R01DK108921, R03 DK106304, and Juvenile Diabetes Research Foundation (JDRF) CDA-2016–189 (to S.A.S); VA Merit award 1 I01 BX003744–01 (to M.G.); NIH R01 DK091526, JDRF Microfluidic-Based Functional Facility at University of Illinois at Chicago, and the Chicago Diabetes Project (CDP) (to J.O., Y.W.); NIH U01 DK070430 and NIDDK/City of Hope Integrated Islet Distribution Program (to A.N.); R01DK67536, R01DK117639 and R01DK103215 (to R.N.K.); JDRF 47–2012-767 and 1-SRA-2014–251-Q-R, NIH R01DK11174 and R01DK117639 (to L.Q.). Y.J. is supported by American Heart Association Scientist Development grant #17SDG33670192 and Michigan Nutrition Obesity Research Center (MNORC) Pilot/ Feasibility grant (P30DK089503). S.S. was an International Student Research Fellow of the Howard Hughes Medical Institute (59107338) and a Helen Hay Whitney Postdoctoral Fellow. L.Q. is the recipient of the Junior Faculty and Career Development Awards from ADA.

REFERENCES

1. Dor Y, Brown J, Martinez OI & Melton DA Adult pancreatic beta-cells are formed by self-duplication rather than stem-cell differentiation. Nature 429, 41–46 (2004). [PubMed: 15129273]
2. Xu X et al. Beta cells can be generated from endogenous progenitors in injured adult mouse pancreas. Cell 132, 197–207 (2008). [PubMed: 18243096]
3. Garofano A, Czernichow P & Breant B Impaired beta-cell regeneration in perinatally malnourished rats: a study with STZ. FASEB J 14, 2611–2617 (2000). [PubMed: 11099480]
4. Teta M, Long SY, Wartschow LM, Rankin MM & Kushner JA Very slow turnover of beta-cells in aged adult mice. Diabetes 54, 2557–2567 (2005). [PubMed: 16123343]
5. Meier JJ et al. Beta-cell replication is the primary mechanism subserving the postnatal expansion of beta-cell mass in humans. Diabetes 57, 1584–1594 (2008). [PubMed: 18334605]
6. Nir T, Melton DA & Dor Y Recovery from diabetes in mice by beta cell regeneration. J Clin Invest 117, 2553–2561 (2007). [PubMed: 17786244]
7. Georgia S & Bhushan A Beta cell replication is the primary mechanism for maintaining postnatal beta cell mass. J Clin Invest 114, 963–968 (2004). [PubMed: 15467835]
8. Okada T et al. Insulin receptors in beta-cells are critical for islet compensatory growth response to insulin resistance. Proc Natl Acad Sci U S A 104, 8977–8982 (2007). [PubMed: 17416680]
9. Golson ML, Misfeldt AA, Kopsombut UG, Petersen CP & Gannon M High Fat Diet Regulation of beta-Cell Proliferation and beta-Cell Mass. Open Endocrinol J 4 (2010).
10. Cox AR et al. Extreme obesity induces massive beta cell expansion in mice through self-renewal and does not alter the beta cell lineage. Diabetologia 59, 1231–1241 (2016). [PubMed: 27003683]
11. Stamateris RE, Sharma RB, Hollern DA & Alonso LC Adaptive beta-cell proliferation increases early in high-fat feeding in mice, concurrent with metabolic changes, with induction of islet cyclin D2 expression. Am J Physiol Endocrinol Metab 305, E149–159 (2013). [PubMed: 23673159]
12. Sachdeva MM & Stoffers DA Minireview: Meeting the demand for insulin: molecular mechanisms of adaptive postnatal beta-cell mass expansion. Mol Endocrinol 23, 747–758 (2009). [PubMed: 19196831]
13. Stewart AF et al. Human beta-cell proliferation and intracellular signaling: part 3. Diabetes 64, 1872–1885 (2015). [PubMed: 25999530]
14. Georgia S et al. Cyclin D2 is essential for the compensatory beta-cell hyperplastic response to insulin resistance in rodents. Diabetes 59, 987–996 (2010). [PubMed: 20103709]
15. Kushner JA et al. Cyclins D2 and D1 are essential for postnatal pancreatic beta-cell growth. Mol Cell Biol 25, 3752–3762 (2005). [PubMed: 15831479]
16. Alonso LC et al. Glucose infusion in mice: a new model to induce beta-cell replication. Diabetes 56, 1792–1801 (2007). [PubMed: 17400928]

17. Lemaitre B, Nicolas E, Michaut L, Reichhart JM & Hoffmann JA The dorsoventral regulatory gene cassette spatzle/Toll/cactus controls the potent antifungal response in Drosophila adults. Cell 86, 973–983 (1996). [PubMed: 8808632]
18. Medzhitov R, Preston-Hurlburt P & Janeway CA Jr. A human homologue of the Drosophila Toll protein signals activation of adaptive immunity. Nature 388, 394–397 (1997). [PubMed: 9237759]
19. Poltorak A et al. Defective LPS signaling in C3H/HeJ and C57BL/10ScCr mice: mutations in Tlr4 gene. Science 282, 2085–2088 (1998). [PubMed: 9851930]
20. Konner AC & Bruning JC Toll-like receptors: linking inflammation to metabolism. Trends Endocrinol Metab 22, 16–23 (2011). [PubMed: 20888253]
21. Shi H et al. TLR4 links innate immunity and fatty acid-induced insulin resistance. J Clin Invest 116, 3015–3025 (2006). [PubMed: 17053832]
22. Donath MY Targeting inflammation in the treatment of type 2 diabetes: time to start. Nat Rev Drug Discov 13, 465–476 (2014). [PubMed: 24854413]
23. Sun S, Ji Y, Kersten S & Qi L Mechanisms of inflammatory responses in obese adipose tissue. Annu Rev Nutr 32, 261–286 (2012). [PubMed: 22404118]
24. Himes RW & Smith CW Tlr2 is critical for diet-induced metabolic syndrome in a murine model. FASEB J 24, 731–739 (2010). [PubMed: 19841034]
25. Razolli DS et al. TLR4 expression in bone marrow-derived cells is both necessary and sufficient to produce the insulin resistance phenotype in diet-induced obesity. Endocrinology 156, 103–113 (2015). [PubMed: 25375037]
26. Vila IK et al. Immune cell Toll-like receptor 4 mediates the development of obesity- and endotoxemia-associated adipose tissue fibrosis. Cell reports 7, 1116–1129 (2014). [PubMed: 24794440]
27. Jia L et al. Hepatocyte Toll-like receptor 4 regulates obesity-induced inflammation and insulin resistance. Nature communications 5, 3878 (2014).
28. Lee CC, Avalos AM & Ploegh HL Accessory molecules for Toll-like receptors and their function. Nat Rev Immunol 12, 168–179 (2012). [PubMed: 22301850]
29. Vikram A & Jena G S961, an insulin receptor antagonist causes hyperinsulinemia, insulin-resistance and depletion of energy stores in rats. Biochem Biophys Res Commun 398, 260–265 (2010). [PubMed: 20599729]
30. Ji Y et al. Diet-Induced Alterations in Gut Microflora Contribute to Lethal Pulmonary Damage in TLR2/TLR4-Deficient Mice. Cell reports 8, 137–149 (2014). [PubMed: 24953658]
31. Michael MD et al. Loss of insulin signaling in hepatocytes leads to severe insulin resistance and progressive hepatic dysfunction. Mol Cell 6, 87–97 (2000). [PubMed: 10949030]
32. Rane SG et al. Loss of Cdk4 expression causes insulin-deficient diabetes and Cdk4 activation results in beta-islet cell hyperplasia. Nat Genet 22, 44–52 (1999). [PubMed: 10319860]
33. Dirice E et al. Soluble factors secreted by T cells promote beta-cell proliferation. Diabetes 63, 188–202 (2014). [PubMed: 24089508]
34. Xiao X et al. M2 macrophages promote beta-cell proliferation by up-regulation of SMAD7. Proc Natl Acad Sci U S A 111, E1211–1220 (2014). [PubMed: 24639504]
35. Jourdan T et al. Activation of the Nlrp3 inflammasome in infiltrating macrophages by endocannabinoids mediates beta cell loss in type 2 diabetes. Nat Med 19, 1132–1140 (2013). [PubMed: 23955712]
36. El Ouaamari A et al. SerpinB1 Promotes Pancreatic beta Cell Proliferation. Cell Metab 23, 194–205 (2016). [PubMed: 26701651]
37. Brissova M et al. Islet microenvironment, modulated by vascular endothelial growth factor-A signaling, promotes beta cell regeneration. Cell Metab 19, 498–511 (2014). [PubMed: 24561261]
38. Terazono K et al. A novel gene activated in regenerating islets. J Biol Chem 263, 2111–2114 (1988). [PubMed: 2963000]
39. Li Q et al. Reg2 expression is required for pancreatic islet compensation in response to aging and high fat diet-induced obesity. Endocrinology, en20161551 (2016).
40. Chen H et al. PDGF signalling controls age-dependent proliferation in pancreatic beta-cells. Nature 478, 349–355 (2011). [PubMed: 21993628]

41. Carboneau BA et al. Opposing effects of prostaglandin E2 receptors EP3 and EP4 on mouse and human beta-cell survival and proliferation. Molecular metabolism 6, 548–559 (2017). [PubMed: 28580285]
42. Wang P et al. Diabetes mellitus--advances and challenges in human beta-cell proliferation. Nature reviews. Endocrinology 11, 201–212 (2015).
43. Crabtree JS et al. Of mice and MEN1: Insulinomas in a conditional mouse knockout. Mol Cell Biol 23, 6075–6085 (2003). [PubMed: 12917331]
44. Imai J et al. Regulation of pancreatic beta cell mass by neuronal signals from the liver. Science 322, 1250–1254 (2008). [PubMed: 19023081]

METHODS-ONLY REFERENCES

45. Darveau RP et al. Porphyromonas gingivalis lipopolysaccharide contains multiple lipid A species that functionally interact with both toll-like receptors 2 and 4. Infect Immun 72, 5041–5051 (2004). [PubMed: 15321997]
46. Ji Y et al. Activation of Natural Killer T Cells Promotes M2 Macrophage Polarization in Adipose Tissue and Improves Systemic Glucose Tolerance via Interleukin-4 (IL-4)/STAT6 Protein Signaling Axis in Obesity. J Biol Chem 287, 13561–13571 (2012). [PubMed: 22396530]
47. Szot GL, Koudria P & Bluestone JA Transplantation of pancreatic islets into the kidney capsule of diabetic mice. Journal of visualized experiments : JoVE, 404 (2007).
48. Zmuda EJ, Powell CA & Hai T A method for murine islet isolation and subcapsular kidney transplantation. Journal of visualized experiments : JoVE (2011).
49. Kamran P et al. Parabiosis in mice: a detailed protocol. Journal of visualized experiments : JoVE (2013).
50. Ricordi C et al. National Institutes of Health-Sponsored Clinical Islet Transplantation Consortium Phase 3 Trial: Manufacture of a Complex Cellular Product at Eight Processing Facilities. Diabetes 65, 3418–3428 (2016). [PubMed: 27465220]
51. Adewola AF et al. Microfluidic perifusion and imaging device for multi-parametric islet function assessment. Biomed Microdevices 12, 409–417 (2010). [PubMed: 20300858]
52. Xing Y et al. A pumpless microfluidic device driven by surface tension for pancreatic islet analysis. Biomed Microdevices 18, 80 (2016). [PubMed: 27534648]
53. Ji Y et al. Short Term High Fat Diet Challenge Promotes Alternative Macrophage Polarization in Adipose Tissue via Natural Killer T Cells and Interleukin-4. J Biol Chem 287, 24378–24386 (2012). [PubMed: 22645141]
54. Sun S et al. IRE1a is an endogenous substrate of endoplasmic-reticulum-associated degradation. Nat Cell Biol 17, 1546–1555 (2015). [PubMed: 26551274]
55. Sha H et al. The ER-associated degradation adaptor protein Sel1L regulates LPL secretion and lipid metabolism. Cell Metab 20, 458–470 (2014). [PubMed: 25066055]

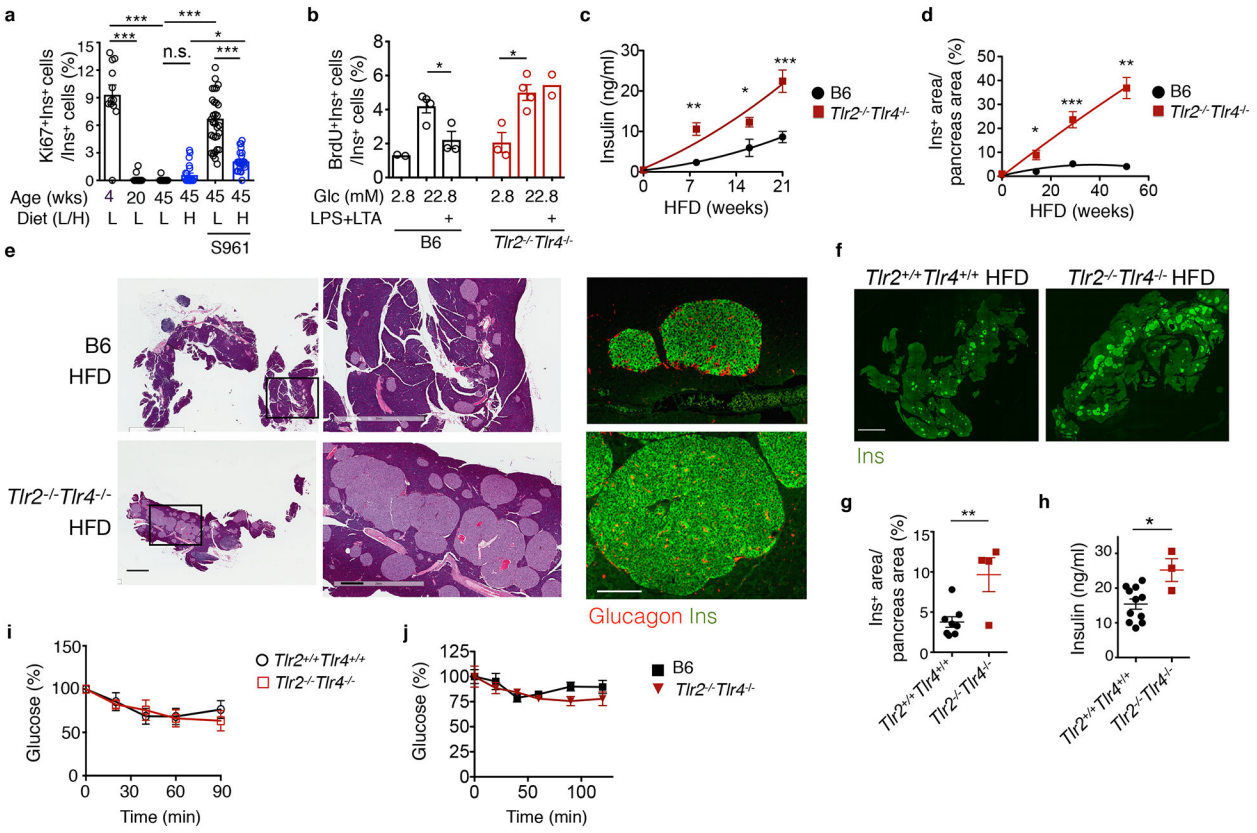

Figure 1. The loss of TLR2 and TLR4 leads to β cell accumulation and hyperinsulinemia in mice on HFD.

a, Flow cytometry analysis of Ki67$^+$ β cells in 4-, 20- or 45-week-old B6 mice fed a LFD (L) or HFD (H, started at 6 weeks of age) for 39 weeks, with or without the insulin receptor antagonist S961 for the last 2 weeks. From left to right, n=12, 13, 16, 23, 32, 26 islets from n=3, 4, 3, 4, 5, 4 mice. **b**, Flow cytometric analysis showing the percent of BrdU$^+$Ins$^+$ β cells in total Ins$^+$ cells in primary B6 and *Tlr2*$^{-/-}$*Tlr4*$^{-/-}$ islets cultured in 2.8 mM (low) or 22.8 mM (high) glucose for 72 hr, with or without LPS+LTA for the last 48 hr. n=9 mice pooled for each genotype. **c**, ELISA showing serum insulin levels of B6 and *Tlr2*$^{-/-}$*Tlr4*$^{-/-}$ mice on HFD for 0, 8, 16 and 21-week starting at 6 weeks of age, after a 5-hr fast. Left to right, n=6, 4, 4, 8 (B6) or 8, 3, 4, 9 mice (*Tlr2*$^{-/-}$*Tlr4*$^{-/-}$). **d**, Quantitation of Ins$^+$ area/pancreas area in B6 and *Tlr2*$^{-/-}$*Tlr4*$^{-/-}$ islets from mice on HFD for 0, 14, 29 and 51 weeks starting at 6 weeks of age, based on immunohistochemical staining of Insulin. Left to right, n=3, 5, 7, 3 (B6) and 3, 6, 3, 3 mice (*Tlr2*$^{-/-}$*Tlr4*$^{-/-}$). **e**, Representative H&E and confocal images showing pancreatic sections (left-middle) and Insulin (Ins)-Glucagon staining of B6 and *Tlr2*$^{-/-}$*Tlr4*$^{-/-}$ mice on HFD for 51 weeks. Scale bars, 2 mm (left), 0.5 mm (middle) and 0.2 mm (right). Representative data from 3 mice each. **f-g**, Representative confocal images showing Ins$^+$ pancreatic areas in *Tlr2*$^{+/+}$*Tlr4*$^{+/+}$ and *Tlr2*$^{-/-}$*Tlr4*$^{-/-}$ littermates on 20-week HFD (**f**), with quantitation of Ins$^+$ areas normalized to total pancreas area shown in (**g**). Scale bars, 2 mm. n=8 and 4 mice (*Tlr2*$^{+/+}$*Tlr4*$^{+/+}$ and *Tlr2*$^{-/-}$*Tlr4*$^{-/-}$). **(h)** ELISA showing serum insulin levels of *Tlr2*$^{+/+}$*Tlr4*$^{+/+}$ and *Tlr2*$^{-/-}$*Tlr4*$^{-/-}$ littermates on 20-week HFD. n=11 (*Tlr2*$^{+/+}$*Tlr4*$^{+/+}$) and 3 mice (*Tlr2*$^{-/-}$*Tlr4*$^{-/-}$). **i-j**, Insulin tolerance test showing changes in

blood glucose levels in *Tlr2*$^{+/+}$*Tlr4*$^{+/+}$ and *Tlr2*$^{-/-}$*Tlr4*$^{-/-}$ littermates (**i**) and B6 and *Tlr2*$^{-/-}$*Tlr4*$^{-/-}$ mice (**j**) on 14-week HFD. n=12 mice each (**i**); n=6 (*Tlr2*$^{+/+}$*Tlr4*$^{+/+}$) and 3 mice (*Tlr2*$^{-/-}$*Tlr4*$^{-/-}$) (**j**). Values represent mean ± SEM. All the data were reproducible with at least two repeats. n.s., not significant; *, p<0.05; **, p<0.01; and ***, p<0.001, using a one-way ANOVA with Newman-Keuls post-test (**a**) or unpaired two-tailed Student's t test (**b-d, g-j**).

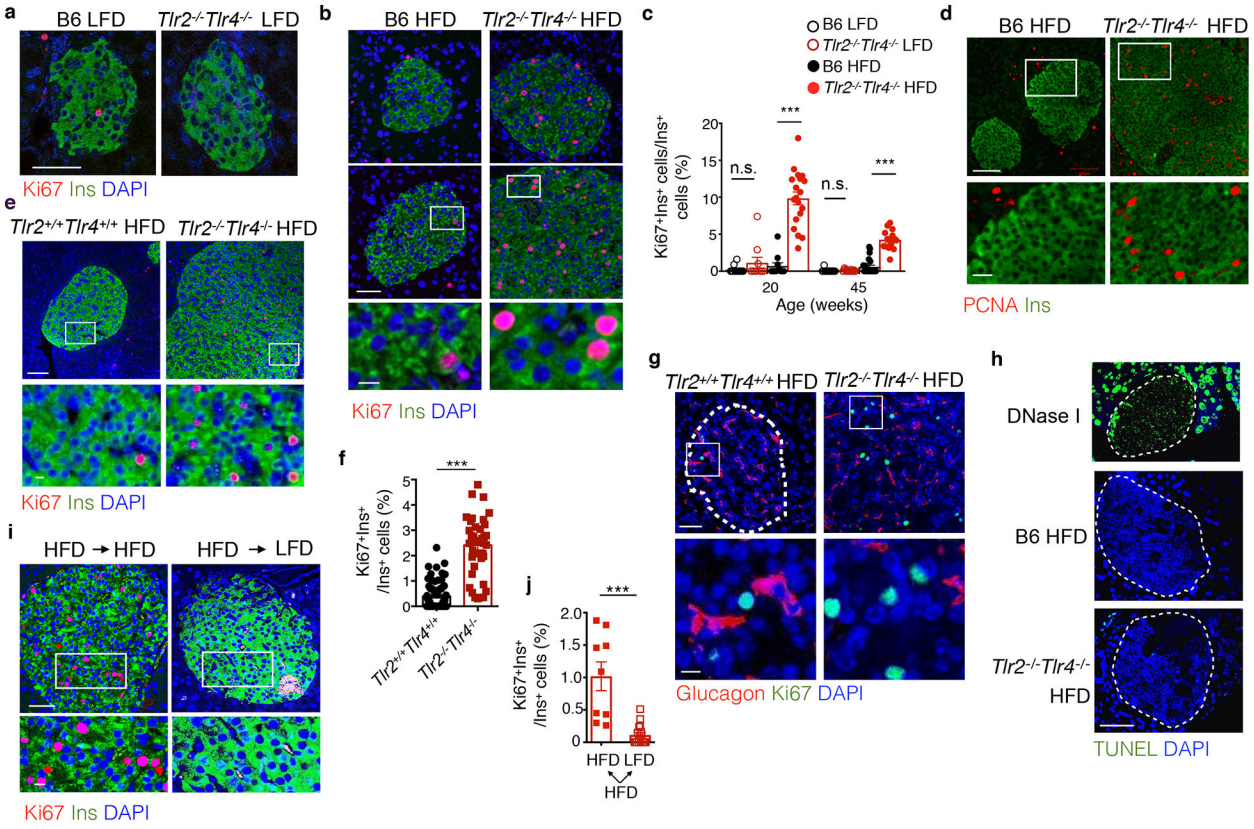

Figure 2. TLR2 and TLR4 deficiency leads to increased β cell proliferation in a HFD-dependent manner.

a-c, Representative confocal images showing Ki67$^+$Ins$^+$ cells in pancreas sections from 20-week-old mice on LFD (**a**) or 14-week HFD (**b**), with quantitation shown in (**c**). Scale bars, 50 μm (**a**), 50 μm (**b**, upper) and 10 μm (**b**, lower). **c**, left to right, n=13, 10, 11, 19, 16, 17, 23, 15 islets from n=4, 4, 5, 6, 3, 3, 3, 3 mice. **d**, Representative confocal images showing PCNA$^+$Ins$^+$ cells in pancreas sections from mice on 29-week HFD. n=3 mice each. Scale bars, 100 μm (upper) and 25 μm (lower). **e-g**, Representative confocal images showing Ki67$^+$Ins$^+$ (**e**) or Ki67$^+$Glucagon$^+$ (**g**) in pancreatic sections from *Tlr2*$^{+/+}$*Tlr4*$^{+/+}$ and *Tlr2*$^{-/-}$*Tlr4*$^{-/-}$ littermates on a 20-week HFD, with quantitation of the percent of Ki67$^+$Ins$^+$ cells in total Ins$^+$ cells shown in (**f**). n=74 islets from 8 *Tlr2*$^{+/+}$*Tlr4*$^{+/+}$ mice and 42 islets from 4 *Tlr2*$^{-/-}$*Tlr4*$^{-/-}$ mice. Scale bars, 50 μm (upper) and 10 μm (lower). **h**, Representative confocal images showing TUNEL assay in pancreas sections from B6 and *Tlr2*$^{-/-}$*Tlr4*$^{-/-}$ mice on 14-week HFD for with DNase I-treated pancreatic section as a positive control. n=3 mice each. Scale bars, 100 μm. **i**, Representative confocal images showing Ki67$^+$Ins$^+$ in *Tlr2*$^{-/-}$*Tlr4*$^{-/-}$ mice fed with HFD for 10 weeks followed by 4 weeks of HFD (left) or LFD (right) feeding. Scale bars, 50 μm (upper) and 10 μm (lower). **j**, Quantitation showing the percent of Ki67$^+$ β cells in *Tlr2*$^{-/-}$*Tlr4*$^{-/-}$ mice on HFD for 32 weeks followed by 4 weeks of either HFD or LFD feeding. Representative images shown in Supplementary Fig. 4g. n=9 (HFD) and 17 (LFD) islets from 3 mice each. Values represent mean ± SEM. All the data were reproducible with at least two repeats. n.s., not significant; ***, p<0.001 by one-way ANOVA with Newman-Keuls post-test (**c**) and two-tailed Student's t test (**f,j**).

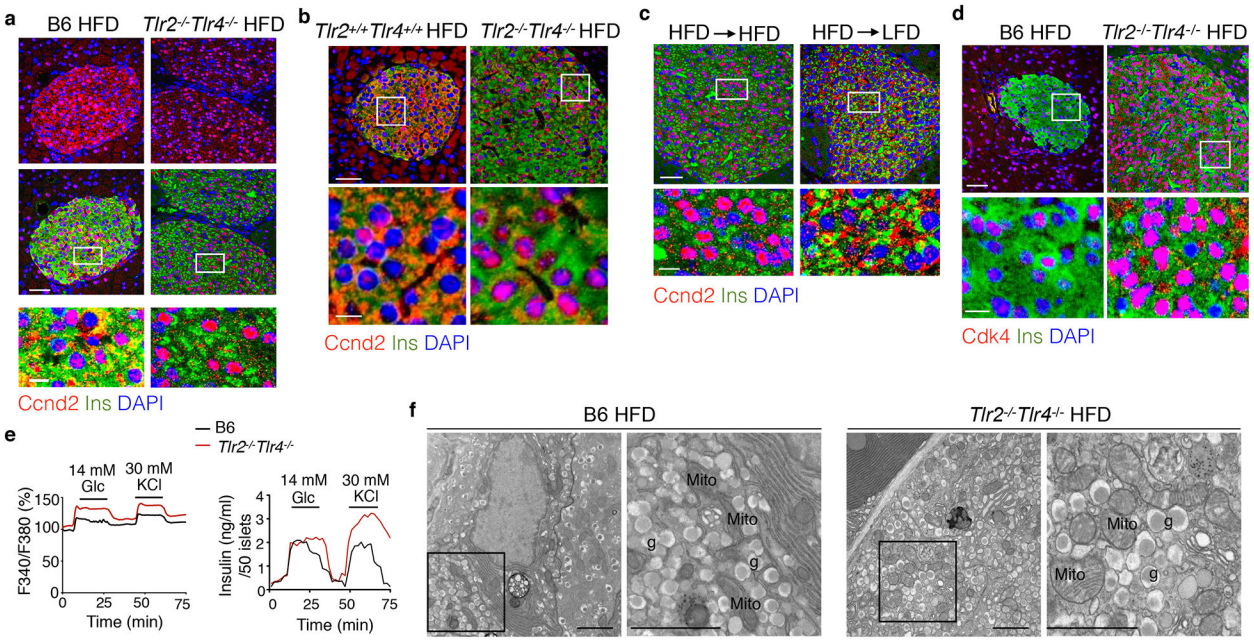

Figure 3. TLR2 and TLR4 deficiency triggers nuclear entry of Ccnd2 in a HFD-dependent manner.

a-b, Representative confocal images showing Ccnd2 localization in Ins$^+$ β cells of (**a**) B6 and *Tlr2*$^{-/-}$*Tlr4*$^{-/-}$ mice on 14-week HFD and (**b**) *Tlr2*$^{+/+}$*Tlr4*$^{+/+}$ and *Tlr2*$^{-/-}$*Tlr4*$^{-/-}$ littermates on 20-week HFD. **c**, Representative confocal images of Ccnd2 localization in Ins$^+$ β cells of *Tlr2*$^{-/-}$*Tlr4*$^{-/-}$ mice on 10-week HFD switched to either LFD or HFD for 4 weeks. **d**, Representative confocal images showing Cdk4 localization in Ins$^+$ β cells of B6 and *Tlr2*$^{-/-}$*Tlr4*$^{-/-}$ mice on 14-week HFD. **a-d**, representative data from 3 mice each with 2 independent repeats. Scale bars, 50 μm (upper) and 10 μm (lower). **e**, Dynamic traces showing calcium signaling (upper) and insulin secretion (lower) of primary islets from B6 and *Tlr2*$^{-/-}$*Tlr4*$^{-/-}$ mice on 9-week HFD stimulated with 20-min 14 mM glucose followed by 15-min 30 mM KCl. Representative data shown from 3 repeats with 50 islets/group. **f**, Representative TEM images showing ultra-structure of β cells from B6 and *Tlr2*$^{-/-}$*Tlr4*$^{-/-}$ mice on 51-week HFD (n=2 mice each, two repeats). mito, mitochondria; g, insulin granules. Scale bars, 2 μm.

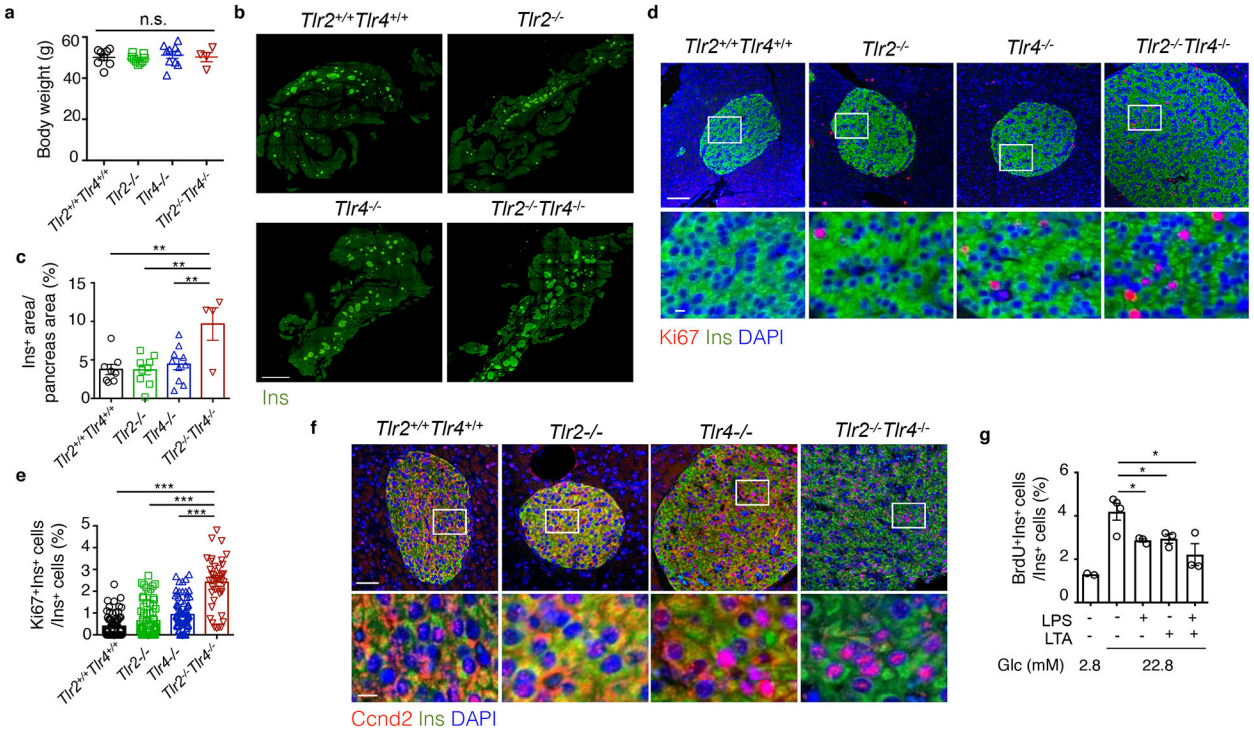

Figure 4. Redundant effect of TLR2 and TLR4 on β cell proliferation.

a-f, Assays using 6-week-old *Tlr2*$^{+/+}$*Tlr4*$^{+/+}$, *Tlr2*$^{-/-}$, *Tlr4*$^{-/-}$ and *Tlr2*$^{-/-}$*Tlr4*$^{-/-}$ littermates on 20-week HFD showing: (**a**) body weight, (**b-c**) representative confocal images of Ins^{+} β cells with quantitation shown in **c** (scale bars, 2 mm), **(d-e)** representative confocal images showing Ki67^{+}Ins^{+} β cells with quantitation shown in **e** (scale bars, 100 μm (upper) and 10 μm (lower))**, (f)** representative confocal images showing Ccnd2 localization in Ins^{+} β cells (scale bars, 50 μm (upper) and 10 μm (lower)). **g**, Flow cytometric analysis showing BrdU^{+} β cells of primary B6 mouse islets cultured in 2.8 mM or 22.8 mM glucose, treated with a combination of LPS and/or LTA for 72 hr. **a-e**, *n*=8, 9,10, 4 mice for *Tlr2*$^{+/+}$*Tlr4*$^{+/+}$, *Tlr2*$^{-/-}$, *Tlr4*$^{-/-}$, and *Tlr2*$^{-/-}$*Tlr4*$^{-/-}$; **e**, *n*=74, 72, 83 and 42 islets for *Tlr2*$^{+/+}$*Tlr4*$^{+/+}$, *Tlr2*$^{-/-}$, *Tlr4*$^{-/-}$, and *Tlr2*$^{-/-}$*Tlr4*$^{-/-}$ mice; **g**, *n*=9 mice. All the data were reproducible with at least two repeats. Values represent mean ± SEM. n.s., not significant; *, p<0.05; **, p<0.01; and ***, p<0.001, by one-way ANOVA with Newman-Keuls post test.

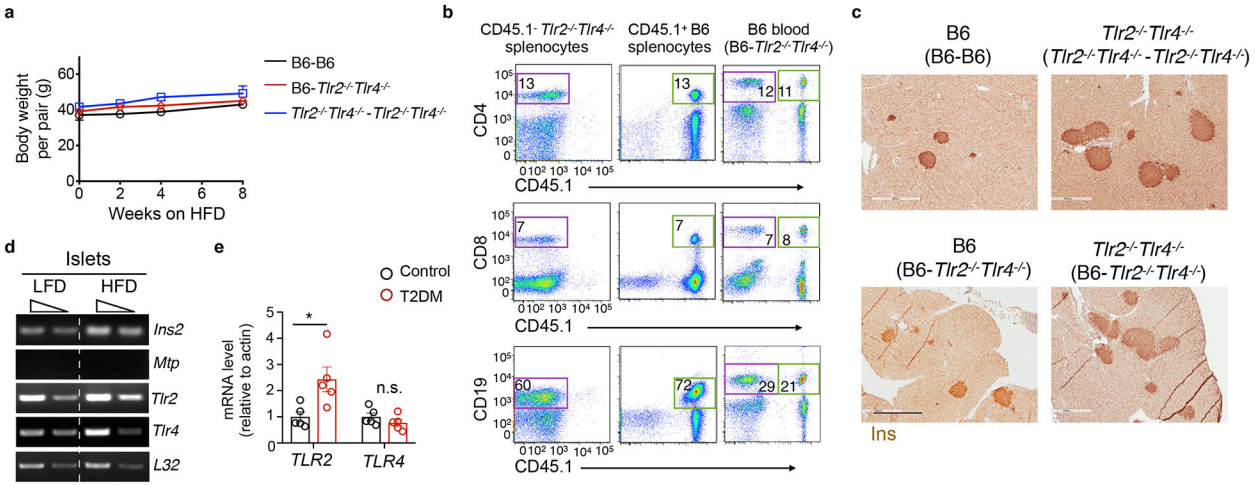

Figure 5. The effect of TLR2 and TLR4 on HFD-induced β cell proliferation is independent of circulating factors.

a, body weight gain of parabiotic pairs on a HFD following the surgery and 3-week recovery. **b**, flow cytometric plots showing the equilibration of $CD4^+$ T cells, $CD8^+$ T cells and $CD19^+$ B cells in the blood of the $CD45.1^+$ B6 - $CD45.1^-$ *Tlr2*$^{-/-}$*Tlr4*$^{-/-}$ parabiotic pairs 3 weeks post-surgery (prior to HFD feeding). Splenocytes from unpaired B6 or *Tlr2*$^{-/-}$*Tlr4*$^{-/-}$ mice were used as controls (left two columns). Number refers to the percent of gated cells in total lymphocytes or splenocytes. (c) Representative images of Ins^+ β cells in pancreatic sections of parabiotic pairs on 14-week HFD. Scale bars, 0.5 mm. **a-c**, *n*=4, 4, 6 mice for B6-B6, *Tlr2*$^{-/-}$*Tlr4*$^{-/-}$ - *Tlr2*$^{-/-}$*Tlr4*$^{-/-}$ pair, and B6-*Tlr2*$^{-/-}$*Tlr4*$^{-/-}$ pairs. **d**, RT-PCR analysis showing *Tlr2* and *Tlr4* expression in islets from B6 mice fed on a LFD or 7-month HFD. Triangles represent a 4-fold dilution of cDNA samples. Islets pooled from 4 mice. Two controls: Mtp, Microsomal triglyceride transfer protein; Ins2, Insulin 2. The gel was cropped to show relevant bands. **e**, qPCR analysis of *TLR2* and *TLR4* expression in human T2D islets vs. healthy islets (n=5 individuals each). Values represent mean ± SEM. n.s., not significant; *, *p*=0.022 by two-tailed Student's *t* test.

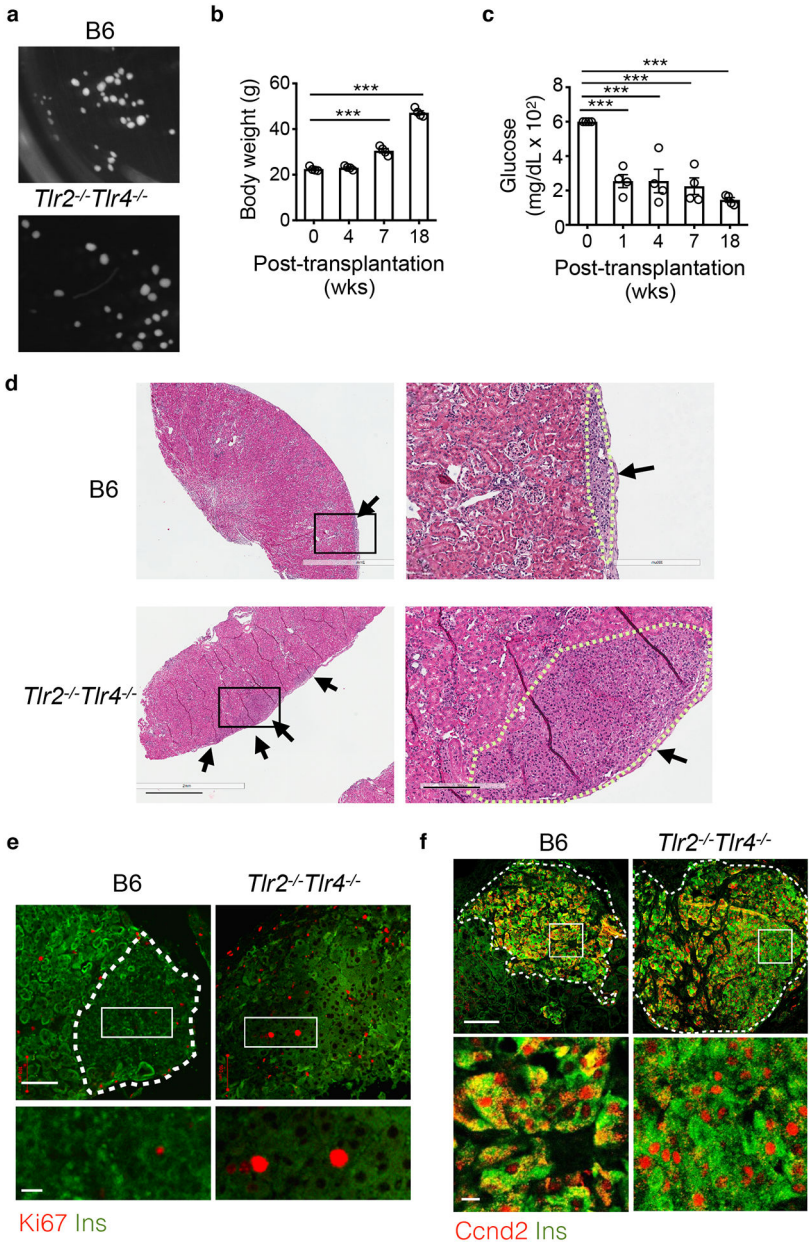

Figure 6. The effect of TLR2 and TLR4 on HFD-induced β cell proliferation is islet intrinsic.

a, Representative light microscopic images showing the size of primary islets from age-matched *Tlr2*$^{-/-}$*Tlr4*$^{-/-}$ and B6 mice on LFD used for transplantation under the kidney capsule. 100 B6 and 100 *Tlr2*$^{-/-}$*Tlr4*$^{-/-}$ primary islets were transplanted under the left and right kidney capsules of the same recipient, either B6 or *Tlr2*$^{-/-}$*Tlr4*$^{-/-}$, respectively. **b-c**, Body weight (**b**) and blood glucose (**c**) of B6 recipients post-transplantation. The same trends were observed for *Tlr2*$^{-/-}$*Tlr4*$^{-/-}$ recipients (n=4; not shown). **d**, Representative H&E images showing islets (arrows) from recipient kidneys received islet grafts from B6 (upper) or *Tlr2*$^{-/-}$*Tlr4*$^{-/-}$ (lower) mice. The dotted line outlines the boundary of the islet grafts. Scale bars, 1 mm (left) and 0.2 mm (right). **e,f**, Representative confocal images showing Ki67^{+}Ins^{+} cells (**e**) or Ccnd2^{+}Ins^{+} (**f**) of transplanted islets under kidney capsules. Scale

bars, 100 μm (upper) and 20 μm (lower inset). The dotted line marks the boundary of the islets (note high auto-fluorescent signals of the surrounding kidney tubules); for *Tlr2*$^{-/-}$*Tlr4*$^{-/-}$ islets, the whole field is full of β cells (**e**). Representative image from 4 mice each with two repeats. Values represent mean ± SEM. ***, $p<0.001$ by two-tailed Student's *t*-test (**b-c**), each compared to day 0.

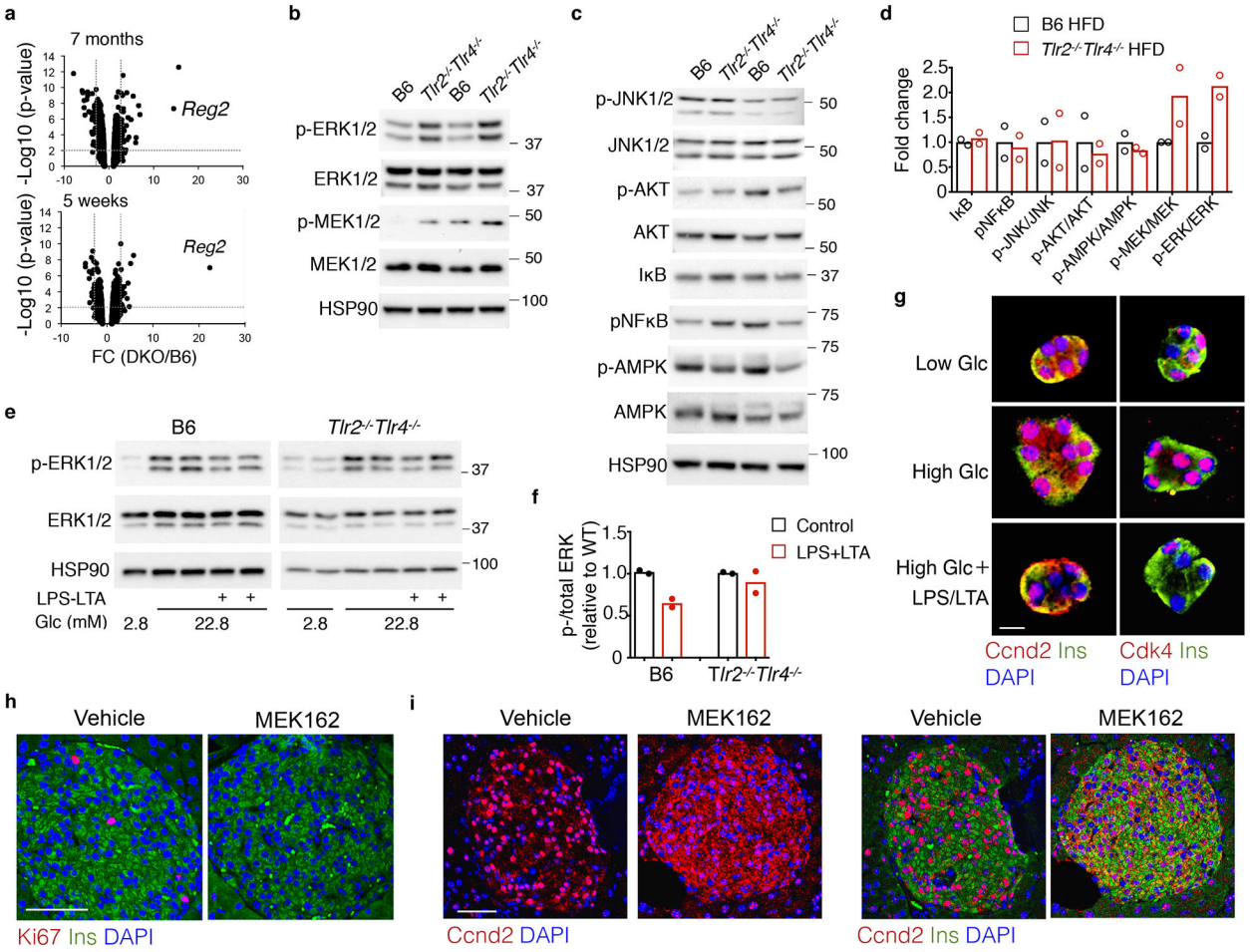

Figure 7. TLR2 and TLR4 inhibit β cell proliferation via the Mek-Erk pathway.

a, Volcano plot analysis of the genome-wide cDNA profiling showing the gene expression change between *Tlr2*$^{-/-}$*Tlr4*$^{-/-}$ and B6 islets on 7-month (upper) and 5-week (lower) HFD. *n*= 4 each for 7-month HFD cohorts, and 2, 4 mice for 5-week HFD *Tlr2*$^{-/-}$*Tlr4*$^{-/-}$ and B6 mice. The y-axis *p* value calculated by IBMT regularized *t* test. **b-d**, Immunoblots showing the expression and phosphorylation of Mek1/2 and Erk1/2 (**b**), and other kinases (**c**) in islets from mice on 40-week HFD, with quantitation of either total protein level or the ratio of phosphorylated- to total protein shown in (**d**). Each lane/dot, pooled islets from 3 mice. **e**, Immunoblots showing the expression and phosphorylation of Erk1/2 in B6 or *Tlr2*$^{-/-}$*Tlr4*$^{-/-}$ islets cultured in 2.8 or 22.8 mM glucose with or without LPS and LTA for 48 hr, with quantitation of phosphorylated- to total protein shown in (**f**). Each lane/dot, pooled islets from 5 mice. **b,c,e**, The gel was cropped to show relevant bands. **g**, Representative confocal images of Ccnd2^{+}Ins^{+} (left) and Cdk4^{+}Ins^{+} in primary islet cells pooled from five 4-month-old B6 mice on a LFD. Islets were dissociated and cultured in 2.8 or 22.8 mM glucose with or without LPS and LTA for 72 hr prior to immunostaining. Individual color channels were shown in Supplementary Figure 8a–b. Scale bars, 10 μm. **h-i**, Representative confocal images of Ki67^{+}Ins^{+} (**h**, with quantitation shown in Supplementary Figure 8f) and Ccnd2^{+}Ins^{+} (**i**) in pancreatic islets of *Tlr2*$^{-/-}$*Tlr4*$^{-/-}$ mice on 8-week HFD treated with MEK162 for 48 hr. n=2 mice for vehicle and 4 mice for MEK162 treatment. Scale bars, 50

μm. **d, f**, Values represent mean ± SEM. All the data were reproducible with at least two repeats.